

**Dlg1 is required for myofibrillar  
arrangement in the *Drosophila* heart**

**Dissertation zur Erlangung des Doktorgrades der Fakultät  
für Biologie der Ludwig-Maximilians-Universität  
München**

**Vorgelegt von  
Diplom-Molekularmedizinerin  
Annette Hellbach  
aus Hanau, Hessen**

**2. Oktober 2013**

## **Ehrenwörtliche Erklärung**

Hiermit erkläre ich, dass ich die vorliegende Dissertation selbstständig und ohne unerlaubte Hilfe angefertigt habe. Ich habe weder anderweitig versucht, eine Dissertation einzureichen oder eine Doktorprüfung durchzuführen, noch habe ich diese Dissertation oder Teile derselben einer anderen Prüfungskommission vorgelegt.

München, den.....  
.....  
(Unterschrift)

Promotionsgesuch eingereicht am: Mittwoch, den 2.10.2013

Rigorosum am: Montag, den 24.2.2014

Erster Gutachter: Prof. Dr. Stefan Jentsch

Zweiter Gutachter: Prof. Dr. Heinrich Leonhardt

Die vorliegende Arbeit wurde von Januar 2010 bis Oktober 2013 unter der Anleitung von Dr. Frank Schnorrer am Max-Planck-Institut für Biochemie in Martinsried bei München durchgeführt.

*Meinen Eltern in Dankbarkeit.*

Der Weltgeist will nicht fesseln uns und engen,  
Er will uns Stuf' um Stufe heben, weiten.

aus „Stufen“ von Hermann Hesse

## Table of contents

<b>1. Summary</b>	<b>1</b>
<b>2. Introduction</b>	<b>2</b>
<b>2.1 Development and morphology of the <i>Drosophila</i> heart</b>	<b>3</b>
2.1.1 Development of the embryonic heart	
2.1.2 Assembly of myofibrils in the larval heart	
2.1.3 Remodeling of the larval into the adult heart	
2.1.4. Adult heart morphology	
<b>2.2 Sarcomeres and myofibrils</b>	<b>9</b>
<b>2.3 Models of myofibrillogenesis</b>	<b>11</b>
<b>2.4 <i>Drosophila</i> as a model system to study heart development</b>	<b>13</b>
<b>2.5 Human cardiomyopathies</b>	<b>15</b>
<b>2.6 The polarity gene <i>Discs large 1 (Dlg1)</i></b>	<b>16</b>
2.6.1 Dlg1 is conserved from <i>Drosophila</i> to humans	
2.6.2 Dlg1 establishes polarity in <i>Drosophila</i> epithelia	
2.6.3 Dlg1 is a tumor suppressor	
2.6.4 Dlg1's role in neurons	
2.6.5 Dlg1's role in muscle	
<b>2.7 The method of RNA interference (RNAi)</b>	<b>20</b>
<b>2.8 Genomic GFP-tagged fosmid clones in the adult <i>Drosophila</i> heart</b>	<b>21</b>
<b>2.9 Aim of this study</b>	<b>23</b>
<b>3. Results</b>	<b>24</b>
<b>3.1 Time course of adult cardiac myofibrillogenesis</b>	<b>24</b>
<b>3.2 Localization of junctional proteins in larval and adult hearts</b>	<b>28</b>
3.2.1 Integrin localizes differentially to the longitudinal cell-cell junction	
3.2.2 Localization of the polarity protein Dlg1 in the <i>Drosophila</i> heart	
<b>3.3 The role of Dlg1 in heart</b>	<b>35</b>
3.3.1 The adult <i>Dlg1</i> loss-of-function phenotype	

3.3.2 The <i>Dlg1</i> phenotype during development	
3.3.3 Cell junctions in <i>Dlg1</i> knock-down hearts	
<b>3.4 Functional investigation of a genomic fosmid library in heart</b>	<b>45</b>
<b>4. Discussion</b>	<b>48</b>
4.1 Loss of <i>Dlg1</i> in heart by RNAi results in major heart defects	48
4.2 Probing the specificity of the <i>Dlg1</i> RNAi phenotype	49
4.3 Dlg1 redirects myofibrils together with integrins	49
4.4 The <i>Dlg1</i> phenotype arises during heart development in larvae and pupae	50
4.5 How does Dlg1 link to integrins?	51
4.6 Comparing cardiac polarity to epithelial polarity	52
4.7 A function for pericardial cells in myofibril organization	52
4.8 Dlg1 and cardiomyopathies	53
4.9 The fosmid library: a valuable resource for <i>Drosophila</i> biology	54
<b>5. Materials and Methods</b>	<b>55</b>
<b>6. References</b>	<b>58</b>
<b>7. Acknowledgements</b>	<b>67</b>

## 1. Summary

Without a beating heart, no higher animal life would be possible on earth. The heart as the central organ of the circulatory system in vertebrates pumps blood through the body and thus transports nutrients and oxygen to all destinations in the body. To fulfill this essential function, the heart requires life-long regular contractions. These are triggered by coordinated actomyosin contractions in each cardiomyocyte. For a controlled systolic contraction of the entire heart, the contractile myofibrils must be arrayed in the proper order in each cardiomyocyte to correctly define the contraction axis of the heart.

During my PhD thesis I made use of the *Drosophila melanogaster* heart to identify genes which are central to myofibrillar arrangement in the heart. Many structural components of vertebrate muscles and heart are conserved in *Drosophila*, which therefore serves as a powerful genetic model system to study heart muscle morphogenesis.

This study demonstrates, that a lack of the polarity gene *Discs large 1 (Dlg1)* causes myofibrillar misarrangement in cardiomyocytes, resulting in a longitudinal instead of the proper circular order of myofibrils. This misarrangement is correlated with mislocalization of the longitudinal  $\beta$ PS integrin pool. Normally, integrin localizes along the longitudinal junction between the two cardiomyocyte rows which form the heart tube. The myofibrils are organized from this longitudinal junction. In *Dlg1* knock-down hearts, the longitudinal  $\beta$ PS integrin pool relocates from the longitudinal to the transverse junction of the cardiomyocytes. As a consequence, the myofibrils which are anchored at this mislocalized integrin pool, are oriented longitudinally instead of circularly around the heart tube. Mechanistically, *Dlg1* is found close to the longitudinal integrin pool and by analogy to its role in epithelia might define the membrane domain in cardiomyocytes that recruits integrins and in turn organizes myofibrils.

In conclusion, *Dlg1* is required for localization of the longitudinal  $\beta$ PS integrin pool in cardiomyocytes, which determines myofibrillar orientation and thus the proper contraction axis of the heart.

## **2. Introduction**

The heart is the central organ of our circulatory system. Without it, blood would stop flowing through our veins and our organs would starve of oxygen and nutrients. This would result in death within minutes.

At rest, the human heart pumps about 60 times per minute, transporting about 5 L of blood. This sums up to 300 L in an hour and 7200 L of blood in a day. In an average life time of 80 years, the heart pumps the incredible amount of 210 million L of blood, which is about the volume of one million bath tubs.

This significant amount of work is produced by a rather small muscle of about 300 grams, the four-chambered human heart. In vertebrates, it derives from the lateral plate mesoderm. Ectoderm, mesoderm and endoderm are the three primordial germ layers of the early embryo. The mesoderm is located in between endoderm and ectoderm. In vertebrates, it can be divided into three subparts: the paraxial, intermediate and lateral plate mesoderm. All skeletal musculature arises from the paraxial mesoderm. However, the circulatory system including the heart is primarily formed by the lateral plate mesoderm. Within the lateral plate mesoderm, two cardiac progenitor populations are specified by the transcription factor Nkx2.5 (Prall et al., 2007): the first heart field and the second heart field (Vincent and Buckingham, 2010). The first heart field differentiates before the second one and builds the precursor of the left ventricle. The second heart field then migrates to the pharyngeal mesoderm and forms the atrial and right ventricular myocardium (Buckingham et al., 2005). It also builds the outflow tract of the heart (Grimes et al., 2010). When the cardiomyocytes of the embryonic heart are assembled, each cardiomyocyte organizes its myofibrils e.g. from the 5-somite stage on in avian embryos in which heartbeat starts at the 9-somite stage (Du et al., 2008). The heart consists of specialized contractile muscle cells called cardiomyocytes. Each cardiomyocyte houses many myofibrils, which consist of linearly arrayed contractile units called sarcomeres.

To achieve heart contractions in a controlled and coordinated way it is essential that the myofibrils in each of the cardiomyocytes are arrayed in a very regular way. Otherwise the contraction axis of the heart would be irregular and pumping ineffective. As myofibrillar organization is essential for heart function, but the molecular mechanism,

how this organization emerges during development, is not very well understood, I decided to tackle this important question during my PhD.

Although *Drosophila* has an open circulatory system, its heart also contracts regularly and continuously throughout the life of the fly. It is built by cardiomyocytes that house regularly arranged myofibrils. Many myofibrillar proteins are conserved from flies to vertebrates (Fyrberg and Goldstein, 1990). Therefore, I used *Drosophila* as a model system to understand how myofibrils are arranged during heart development.

## **2.1 Development and morphology of the *Drosophila* heart**

### **2.1.1 Development of the embryonic heart**

In *Drosophila*, the cardioblasts form two rows of cells below the dorsal epidermis, one on the left and one on the right side of the embryo. During embryonic dorsal closure, the two cardioblast rows move towards each other and adhere together at stage 16. Afterwards, cardioblasts differentiate into cardiomyocytes and form a central lumen in the middle of the heart tube. This tubular heart is located inbetween thoracic segment T3 and abdominal segment A7 and is subdivided into two functional parts: the anterior aorta and the heart proper which is located at the posterior end in abdominal segments 5-7 (Fig. 1) (Monier et al., 2005). The heart proper possesses two relatively large chambers whereas the aorta is thinner in diameter and a subdivision into chambers is lacking (Fig. 1) (Monier et al., 2005; Zeitouni et al., 2007).

Embryonic heart specification is relatively well studied. Early during development, the inductive signal required for cardiac fate specification is sent out from the ectoderm to the underlying mesoderm (Zaffran, 2002). This signal activates a large array of transcription factors which induces cardioblast specification within the cardiac mesoderm, among them NK homeodomain proteins, GATA and T-box factors (Zaffran, 2002). The prototype of NK homeodomain transcription factors is Tinman (Tin) which was first identified in *Drosophila*. Tin is absolutely essential for heart development as *tin* mutants lack a heart. In *Drosophila*, it is expressed after mesoderm invagination, and becomes restricted to the cardioblasts at embryonic stage 10, which induces their differentiation (Zaffran, 2006). Each segment contains two rows of six cardioblasts. Two cardioblasts per segment will differentiate into *seven-up(svp)*-positive ostia cells, the

future hemolymph inflow tracts (Molina and Cripps, 2001). The remaining four will differentiate into cardiomyocytes. *tin* expression stays activated in contractile cardiomyocytes throughout the entire life of the fly (Reim and Frasch, 2010). One important target of Tin is the bHLH transcription factor Hand, which is activated in all cardioblasts as well as pericardial cells at stage 12 and, similar to *tin*, is not switched off anymore (Kölsch and Paululat, 2002; Han, 2005; Sellin et al., 2006). Therefore, a *Hand* enhancer can be used to drive gene expression in cardiomyocytes.

The Ultrabithorax complex genes *Antp*, *Ubx* and *abd-A* control the anterior-posterior patterning of the heart, subdividing it into a dorsal vessel in T3-A4 and the heart proper which is located in A5-A7 (Lo et al., 2002; Perrin et al., 2004). *Antp* is expressed in cardioblasts of the segment T3, whereas *Ubx* expression is restricted to A1-A4. Expression of *abd-A* in the cardioblasts of the segments A5-A7 perfectly matches with the location of the heart proper (Fig. 1).

In order to form a heart tube, the two rows of cardioblasts have to migrate during development. The extracellular matrix (ECM) protein Slit and its receptor Robo are important for this migration, and the later steps of adhesion and lumen formation (Qian et al., 2005; Santiago-Martínez et al., 2006). During migration, *robo* controls the distance between dorsally migrating cardioblasts and the midline. At the dorsal destination, these mesenchymal cells then transit to an epithelial-like character and adhere to each other. At this point, Robo is concentrated at the dorsal longitudinal cell-cell junction and is required for cell-cell attachment (Qian et al., 2005). Attachment starts at the dorsal side of the cardioblasts and only later the tube closes ventrally forming a central lumen (Medioni et al., 2008). These two cell-cell junctions are from now on referred to as the longitudinal junctions which are running from anterior to posterior along the heart tube (Fig. 1).

Both longitudinal and transverse junctions contain E-cadherin and the polarity protein Discs large 1 (Dlg1) (Haag et al., 1999; Qian et al., 2005), mediating stable cell-cell adhesion of the two cardiomyocyte rows.

In conclusion, the embryonic heart is formed by two rows of cardiomyocytes that are attached to each other and face a central lumen. Each segment contains four *tin*- and two *svp*-positive cells (Fig. 1). Myofibrils are not yet present within the cardiomyocytes.

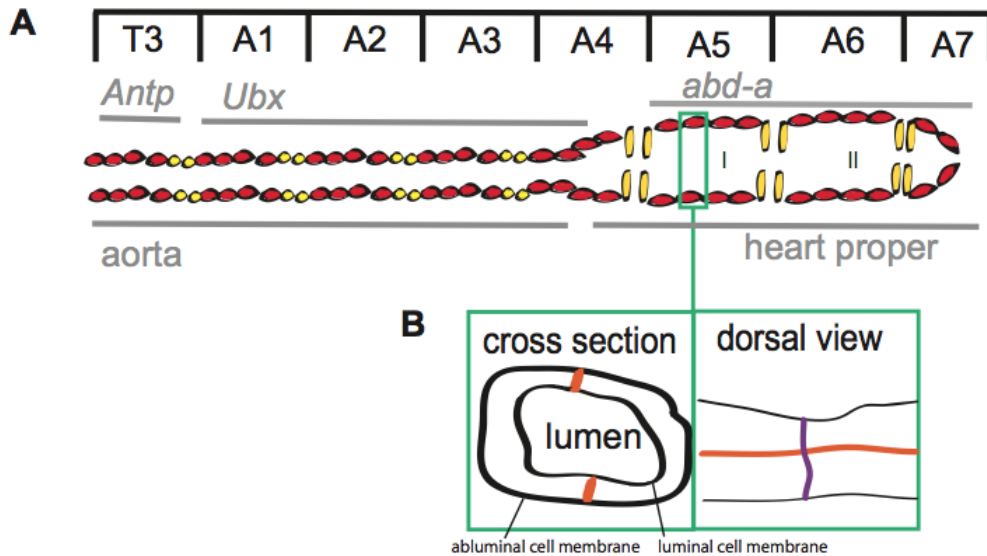


**Figure 1 The embryonic *Drosophila* heart**

(A) The anterior portion of the embryonic heart (aorta) is located in thoracic segment T3 to abdominal segment A4 and built by contractile cardiomyocytes (red) and ostia precursor cells (yellow). The aorta expresses the homeobox genes *Antp* and *Ubx*. The posterior portion or heart proper is located in A5-A7, expresses *abd-a* and forms two chambers (I, II). (B) In the left green box, the longitudinal cell-cell junction (orange, shown in a cross section) which is located between the cells of the opposing rows of cardiomyocytes both on the ventral and dorsal side of the heart tube is shown. The luminal and abluminal cell membranes are indicated as well. In the right green box, the so-called transverse junctions between the neighbouring cardiomyocytes within a row (purple) are depicted in a dorsal view. (modified from Monier et al., 2005)

### 2.1.2 Assembly of myofibrils in the larval heart

At the end of embryogenesis, the heart does not yet beat as it first requires assembly of its contractile myofibrils. During larval development, the heart grows significantly in size without the addition of new cells. Each cardiomyocyte grows larger and assembles its myofibrils. They orient circularly around the heart tube, originating at the longitudinal cell-cell contacts (Fig. 2). In the aorta part of the heart (T3-A4), relatively few myofibrils are built, whereas the heart proper (A5-A7) contains more myofibrils and is beating during all larval stages. Mechanistically, it is unclear how larval myofibrillogenesis is controlled and how the circular arrangement of the myofibrils is achieved.

### 2.1.3 Remodeling of the larval into the adult heart

During pupal metamorphosis, the larval body plan is restructured into the adult body plan. The heart similar to all other tissues undergoes dramatic morphological changes (Monier et al., 2005). The larval heart proper located in abdominal segments A5 to A7 is histolysed and its cardiomyocytes undergo apoptosis (Fig. 2 A, C). The remaining cardiomyocytes of the aorta are remodelled to eventually form four distinct chambers in the adult. No new cells are added (Monier et al., 2005). During remodeling, the heart stops beating and larval myofibrils are degraded. At about 30h APF, adult myofibrils start to develop concomitantly with a further growth of the cardiomyocytes, possibly because they house a larger number of myofibrils compared to the larval heart. As in the larval heart, myofibrils are anchored at the longitudinal cell-cell junction between the two cardiomyocyte rows and run circularly around the tube (Monier et al., 2005). Thus, myofibril contraction reduces the diameter of the lumen and pumps hemolymph out of the heart.

Cardiac remodeling is at least in part controlled by *Ubx*. *Ubx* is expressed in all larval cardiomyocytes in A1 to A4 but becomes restricted to a pair of *svp*-expressing cardiomyocytes at about 30h APF. These *Ubx*- and *svp*-positive cardiomyocytes will differentiate into ostia cells. If *Ubx* is misexpressed in the *tin*-positive contractile cardiomyocytes their morphogenesis is severely disrupted including myofibrillar organization which leads to longitudinal myofibrils (Monier et al., 2005).

At the same time, another Hox gene, *abd-A*, is restricted to the posterior end of the heart in A5, organizing the terminal part of the heart. If it is misexpressed in all cardiomyocytes, again myofibrils orient longitudinally instead of circularly (Monier et al., 2005). However, it is unclear, what the cause for this misarrangement is. In addition to *Ubx* and *abd-A* activity, ecdysone signaling is required in the cardiomyocytes for their remodeling (Monier et al., 2005).

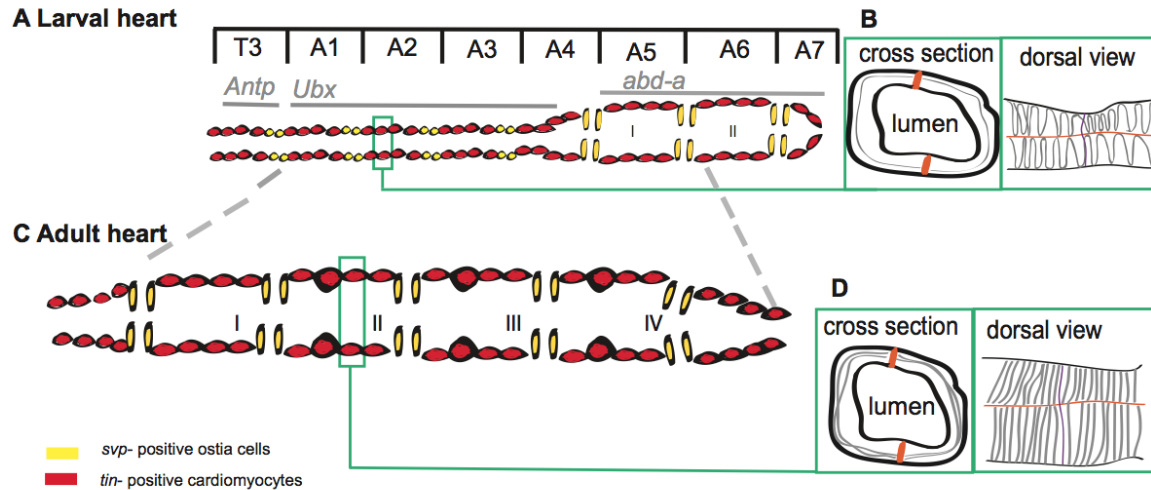


**Figure 2 Scheme of the larval and adult heart**

(A) The posterior portion of the larval heart (heart proper) is built by contractile cardiomyocytes (red) with only a few myofibrils (B, grey). (C) During metamorphosis, larval aorta cells are remodeled: Larval myofibrils are degraded and adult ones (grey) built up (D). The adult heart consists of four chambers (I-IV). *tin*-expressing contractile cardiomyocytes are shown in red, the bigger ones are valve cells. *svp*-expressing ostia cells, hemolymph inflow tracts, are depicted in yellow. (modified from Monier et al., 2005)

In 2007, Zeitouni and colleagues identified several signaling pathways that are involved in the morphological remodeling of the larval to adult heart during metamorphosis. They performed whole genome expression profiling from dissected pupal hearts at eight different time points during cardiac remodeling and demonstrated that the Wnt signaling pathway is involved in ostia differentiation and formation of the posterior end of the heart. Interestingly, block of Wg signaling leads to longitudinal instead of circular myofibrils as well (Monier et al., 2005; Zeitouni et al., 2007). Finally, cardiac valves differentiate from one of the four *tin*-expressing cardiomyocytes in a PDGF-VEGF dependent manner (Fig. 2C) (Zeitouni et al., 2007).

Together, these studies have shown that the gain of circular myofibrils during pupal development is intimately linked to proper heart remodeling. However, the cell biological mechanism how these myofibrils become organized is unclear.

#### 2.1.4 Adult heart morphology

The finally differentiated adult *Drosophila* heart consists of two opposing rows of cardiomyocytes that shape the heart tube (Fig. 2 C, D). Each row is characterized by a sequence of six cardiomyocytes per segment, four being *tin*-positive and contractile, followed by two inflow tract building *svp*-positive ostial cells. One of the *tin*-positive cardiomyocytes differentiates into a special valve cell at three positions in the heart that regulate blood flow and divide the heart into four chambers (Lehmacher et al., 2012). 40-50 pericardial cells are located next to the adult heart and fulfill nephrocyte-like functions (Lehmacher et al., 2012). In addition to the large gain of myofibrils, the adult cardiomyocytes also contain many more mitochondria than at earlier developmental stages. Furthermore, ventral longitudinal muscles of somatic origin form beneath the heart tube during pupal development (Lehmacher et al., 2012).

Within each cardiomyocyte, the sarcoplasmic reticulum is important for excitation-contraction-coupling because it stores calcium ions and releases them in case of muscle contraction (Fig. 3) (Sipido et al., 2012). In the *Drosophila* heart, the sarcoplasmic reticulum is located in close proximity to the myofibrillar A-bands and the Z-discs (Fig. 4B, Fig. 5) (Lehmacher et al., 2012). Together with invaginations of the cardiomyocyte membrane, termed T-tubules, the sarcoplasmic reticulum builds typical morphological structures called dyads (Fig. 4B) (Lehmacher et al., 2012).

The bar-domain protein amphiphysin is the most important marker of the T-tubular system and was shown to be crucial to the correct organization of the T-tubules as well as the closely located sarcoplasmic reticulum (Razzaq, 2001). In rat cardiac muscle, the T-tubular system displays a high complexity and occupies a cell volume of 3.6% (Soeller and Cannell, 1999). As in *Drosophila*, rat and mouse cardiac T-tubules are closely associated with the sarcoplasmic reticulum (Sipido et al., 2012).

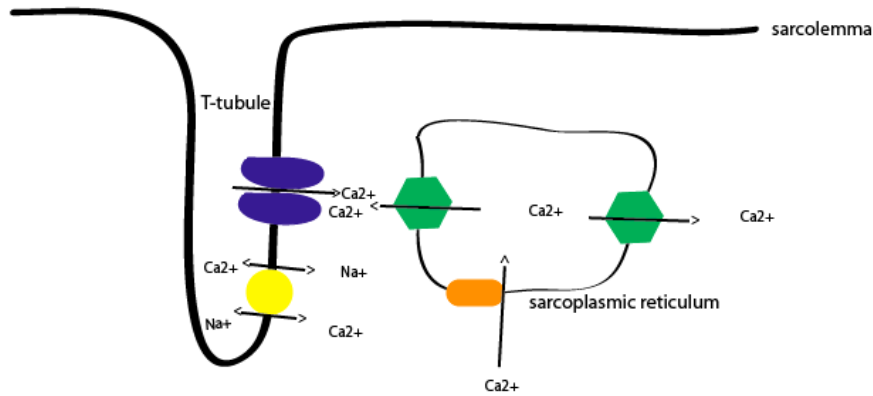


**Figure 3 The calcium cycle in a cardiac ventricular myocyte**

T-tubules reach far down into the cardiomyocyte and are associated with the sarcoplasmic reticulum (SR). In case of a contraction, extracellular calcium enters the cytoplasm via the L-type calcium channel (blue) and from the SR via ryanodine receptors (green). Afterwards, calcium is pumped into the T-tubule by NCX (yellow) and back into the SR by the ATP-driven calcium pump SERCA (orange). (modified from Sipido et al., 2012)

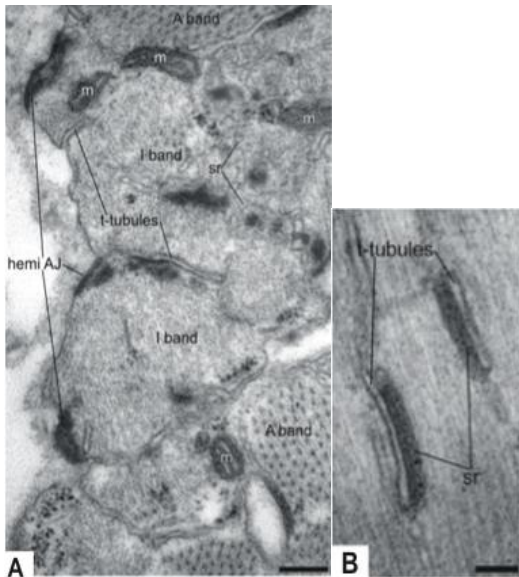


**Figure 4 Cardiomyocyte ultrastructure of adult *Drosophila***

(A) is a sagittal section through the adult T-tubular system which reaches far into the sarcomere. sr= sarcoplasmic reticulum, AJ= adherens junction (B) Dyad-forming T-tubules and SR. (from Lehmacher et al., 2012)

## 2.2 Sarcomeres and myofibrils

The sarcomere is composed of a complex protein machinery which builds the smallest contractile unit of any muscle cell. It consists of an assembly of the thin actin filament

and the thick myosin filament (Fig. 5). The tropomyosin as well as the troponin complex are associated with the thin filaments. Actin filaments are anchored and cross-linked at the so-called Z-disc, where the giant protein titin and the actin cross-linker  $\alpha$ -actinin are located (Sparrow and Schöck, 2009). Vertebrate titin spans the entire thin filament and ends at the M-line, which divides the sarcomere into two identical halves. Titin was found to be essential as a template for sarcomere assembly and the ordered integration of all proteins into the sarcomeric cytoarchitecture (Person et al., 2000). Myosin filaments are located between the thin filaments. The myosin heads can bind to the actin filaments and move to the actin plus end. Thus myosin is responsible for sarcomere contraction via the sliding filament mechanism (Huxley and Hanson, 1954).

The sarcomere's region exclusively covered by thin filaments is called I-band and the one occupied by thick filaments is called A-band (Fig. 5) (Sparrow and Schöck, 2009). Lehmacher and colleagues also defined common features of the sarcomere in larval and adult *Drosophila* cardiomyocytes. The A-band has a size of about 1 $\mu$ m. Z-discs are not always continuous throughout the sarcomere. H-zones and M-lines (Fig. 5) are not obvious at an electron-microscopic level, suggesting that sarcomere regularity is less defined compared to skeletal muscle.

Sarcomeres assemble linearly into myofibrils and thereby build repetitive units. These myofibrils are anchored at the muscle cell membrane, run through the whole muscle cell and reduce it in size when they are contracting.

As mentioned earlier, the muscle cell membrane, also known as sarcolemma, shows typical T-tubular invaginations and is connected to the myofibrils, mostly at their Z-discs. These sarcolemma-myofibril-adhesion sites are termed costameres. At costameres, myofibrils are linked to the extracellular matrix (ECM) by integrins which bind directly to the ECM and are intracellularly linked to Z-disc proteins via intracellular integrin adaptors (Quach and Rando, 2006; Legate et al., 2009). Since costameres connect to the myofibrillar Z-disc, integrin appears in a striated pattern at the sarcolemma (Volk et al., 1990). Especially in older cultured rat cardiomyocytes, costameres are shown to be the sites of force transmission between the Z-discs and the ECM (Danowski et al., 1992).

Apart from this costameric adhesion along the length of the myofibril, myofibrils are anchored at their ends, either in myotendinous junctions, where the muscle connects to its tendon, or, in the case of heart musculature, at the intercalated disc (Fig. 6, 7) (Forbes and Sperelakis, 1985). The intercalated disc is the typical junction between cardiac muscle cells (Fig. 6, 7) (Forbes and Sperelakis, 1985; Franke et al., 2006; Capetanaki et al., 2007). Three types of cell junction complexes can be found in the intercalated disc region in mammals: desmosomes, gap junctions and adherens junctions (Perriard et al., 2003). Hemidherens junctions can be found in the adult *Drosophila* heart, too (Lehmacher et al., 2012).

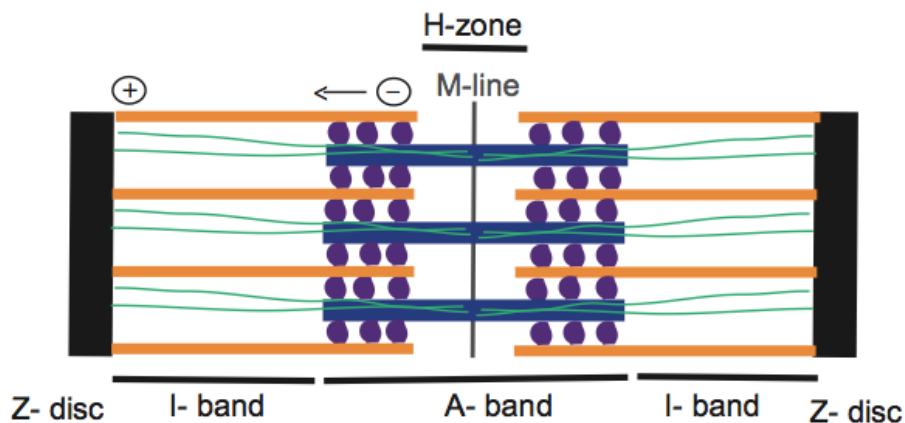


**Figure 5 Sarcomere structure**

The sarcomere is built by two Z-discs (black) to which actin filaments (orange) are anchored. Myosin filaments (blue) are connected to actin filaments by myosin heads (purple). The giant protein titin (green) provides the sarcomere with stability. The sarcomere can be divided into A- band, I- band, M- line, and H- zone.

### 2.3 Models of myofibrillogenesis

Studies both in vivo and in vitro (Dlugosz et al., 1984; Holtzer et al., 1997) have been undertaken to answer the question how myofibrils are formed and several models have been developed based on the experimental findings. The premyofibril model of myofibrillogenesis is supported by data from chick cardiomyocytes, quail cardiomyocytes, *Drosophila* flight muscle and *C. elegans* body wall muscle and thus could apply to other species and muscles as well (Fig. 8) (Du et al., 2008; Sparrow and

Schöck, 2009). First, premyofibrils can be seen close to the membrane where the process of myofibrillogenesis starts (Tokuyasu, 1989). Z-bodies, the Z-disc precursors, develop as aggregation sites for the earliest Z-disc marker  $\alpha$ -actinin as well as titin. The integrin-associated proteins talin and vinculin also appear in a striated pattern along the sarcolemma at an early stage of myofibrillogenesis (Fujita et al., 2007). It is possible that these protocostameres function as docking sites for the premyofibril-associated Z-bodies (Sparrow and Schöck, 2009). Second, nascent myofibrils containing both non-muscle myosin II and muscle-specific myosin II arise (Du et al., 2008). During the third and last step, nascent myofibrils develop into mature ones by completely exchanging non-muscle myosin II by muscle myosin (Du et al., 2008). By this time, Z-bodies have also matured into Z-discs and sarcomeres have reached their mature size. Similar results could be shown in cardiomyocytes from quail precardiac mesoderm explants in cell culture (Du et al., 2003). Also, scaffolding proteins and chaperones might be involved in myofibrillogenesis. For example, N-RAP most likely helps the assembly of actin and  $\alpha$ -actinin into I-Z-I structures early in assembly (Crawford and Horowitz, 2011).

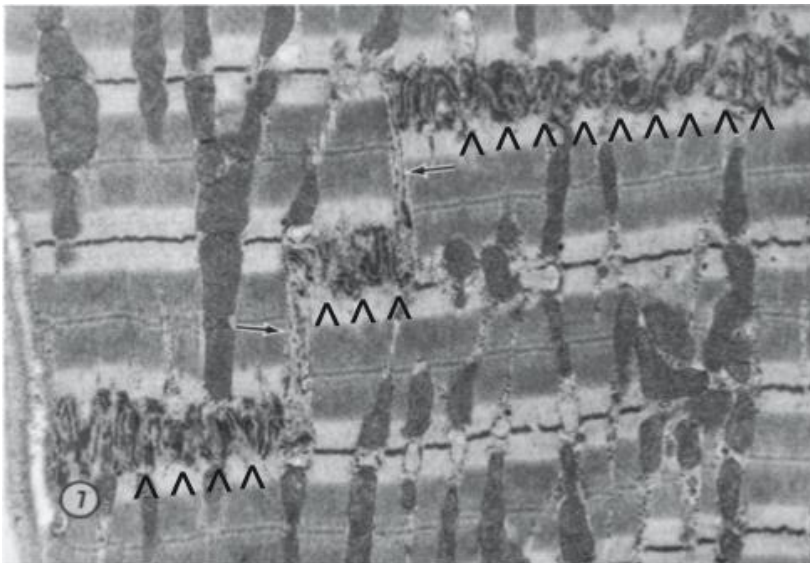


**Figure 6 The intercalated disc in a Rhesus monkey cardiomyocyte**

Electron-microscopic picture of the ventricular septum in a Rhesus monkey. The intercalated disc (arrowheads) can be seen as the border between the two depicted muscle cells and is arranged in a step-like fashion (arrows). (from Forbes and Sperelakis, 1985)

## 2.4 *Drosophila* as a model system to study heart development

*Drosophila* is a well-suited model system to study heart development and insights are often relevant to mammalian heart biology (Na et al., 2013).

Both cytoskeletal proteins that build the contractile filaments of the cardiomyocytes and developmental cardiac transcription factor networks that pattern the heart are well conserved between *Drosophila* and vertebrates (Reim and Frasch, 2010).

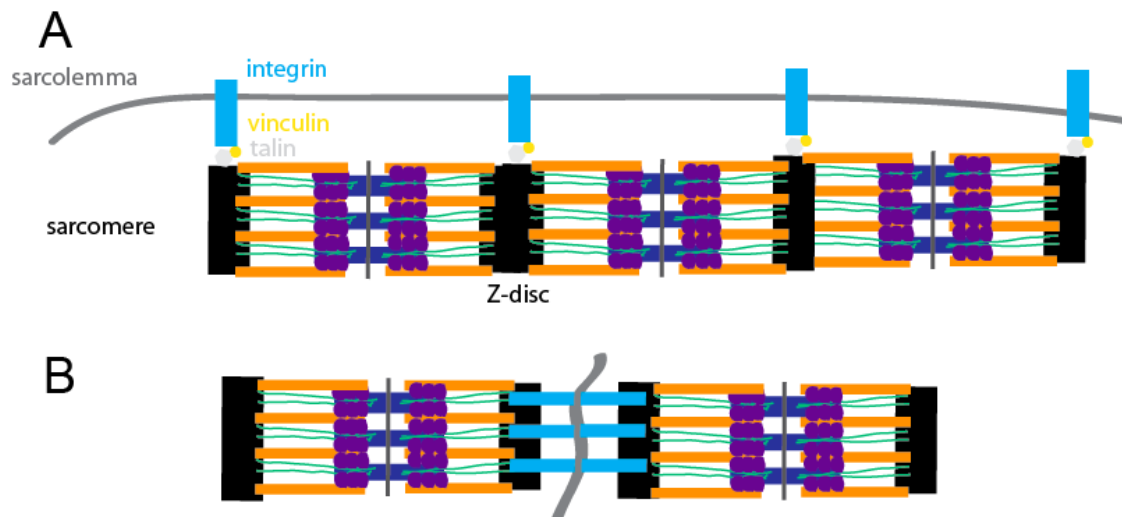


**Figure 7 The costamere and the intercalated disc**

(A) The region and protein complex where myofibrils are anchored to the plasma membrane (sarcolemma in muscles) (dark grey) is termed costamere. Integrins (blue) and molecules associated like talin (light grey) and vinculin (yellow) are located close to the sarcomere's Z-disc (black). In B, the intercalated disc is shown, with the Z-disc (black) connecting to the sarcolemma (dark grey) via integrin (blue). (adapted from Capetanaki et al., 2007; Lehmacher et al., 2012 and Hellbach and Schnorrer, in preparation)

Furthermore, the ultrastructure of the adult *Drosophila* heart reveals analogy to the mammalian heart (Lehmacher et al., 2012). It possesses an intricate T-tubular system which reaches far down into the cardiomyocyte, a sarcoplasmic reticulum, valve cells, and a very similar myofibrillar and sarcomeric structure.

The important cytoskeletal muscle components actin, myosin, titin, and integrins are conserved and fulfill similar functions as their vertebrate counterparts (Fyrberg and Goldstein, 1990).

The transcription factor genes *Hand*, *Mef2*, and *tin*, among others, are also conserved which all play important functional roles both in *Drosophila* and human heart development (Reim and Frasch, 2010).

In conclusion, understanding the mechanism of myofibrillogenesis in the fly heart can also contribute to a better understanding of the vertebrate heart.

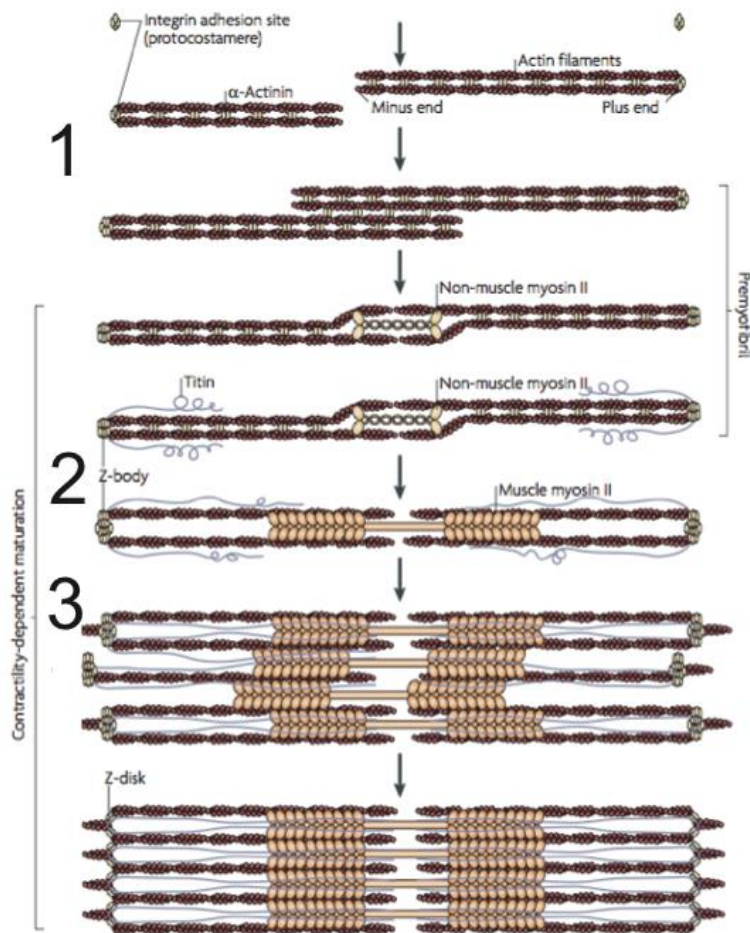


**Figure 8 Model of myofibrillogenesis**

Step 1 shows the polymerization of integrin adhesion sites which are located randomly throughout the muscle cell membrane together with actin filaments. Then, these first actin filaments get connected by  $\alpha$ -actinin and are called premyofibrils into which non-muscle myosin II incorporates and displaces  $\alpha$ -actinin. Now, the contractility-dependent maturation of the myofibrils begins.  $\alpha$ -actinin then becomes restricted to a certain morphological structure which it forms together with the giant molecule titin: the Z-body. Premyofibrils become nascent myofibrils by adding muscle myosin II (step 2). Finally, non-muscle myosin becomes completely substituted by muscle myosin and the Z-bodies move towards each other and build one continuous Z-disk and a mature myofibril (step 3). (adapted from Sparrow and Schöck, 2009)

## 2.5 Human cardiomyopathies

Many diseases affect cardiac morphology and function in humans. These cardiomyopathies can either be inherited or spontaneous. The two most frequent types include hypertrophic cardiomyopathy (HCM) and dilated cardiomyopathy (DCM) with the latter affecting the majority of people suffering from cardiomyopathy (Sussman et al., 1998; Parvari and Levitas, 2012).

HCM is characterized by hypertrophy of the left ventricle as well as myofibrillar disarray (Parvari and Levitas, 2012). The most frequent genetic mutations causing HCM are within the gene of the cardiac  $\beta$ -myosin heavy chain (Geisterfer-Lowrance et al., 1990) and within genes encoding  $\alpha$ -tropomyosin and cardiac troponin T (Thierfelder et al., 1994). Other mutations cover genes for cardiac troponin I and cardiac troponin C,  $\alpha$ -cardiac actin, regulatory myosin light chain, cardiac myosin-binding protein C, titin, and several Z-disc proteins (Morimoto, 2007). This list demonstrates the importance of the sarcomeric components for healthy cardiac morphology and function.

DCM, the most common form of cardiomyopathy, involves an enlargement of the left ventricle and, consequently, a decreased systolic performance (Sussman et al., 1998; Parvari and Levitas, 2012). It mostly leads to sudden death (Parvari and Levitas, 2012). In some cases, DCM also leads to cellular and myofibrillar disarray (Beltrami et al., 1995; Perriard et al., 2003). Five percent of DCM cases are inherited and the majority of genes encode for sarcomeric proteins or components that are otherwise involved in force generation, like for example constituents of the costamere (Parvari and Levitas, 2012). Some evidence exists that proteins of the intercalated disc might be involved in the pathogenesis of DCM as well (Perriard et al., 2003).

The importance of the sarcomeres is being emphasized by the severe effects of cardiomyopathy cases in which sarcomeric genes are mutated. Similarly, proper myofibrillar arrangement shows to be inevitable for heart function since some cardiomyopathies are characterized by a chaotic myofibrillar arrangement (Beltrami et al., 1995; Perriard et al., 2003). Myofibrils are anchored at the intercalated disc in the mammalian heart (Noorman et al., 2009). However, it is unknown how this anchoring

site for myofibrils is established and how it distinguishes itself from other spaces within the cell membrane.

I hypothesized, that the spatial identification of the myofibril anchoring point, which is the longitudinal cell-cell junction between the two opposing cardiomyocyte rows in *Drosophila* and the intercalated disc in mammals, might be defined by proteins with essential functions in epithelial polarity. Therefore, I investigated the function of *Discs large 1 (Dlg1)* which was formerly identified in a muscle-specific screen in the lab (Schnorrer et al., 2010).

## 2.6 The polarity gene *Discs large 1 (Dlg1)*

### 2.6.1 Dlg1 is conserved from *Drosophila* to humans

Discs large 1 (Dlg1) belongs to the membrane-associated guanylate kinases (MAGUK) (Anderson, 1996). Dlg1 shares with other family members its one PDZ, one SH3, and one GuKc domain, but in addition possesses another two PDZ domains (Fig. 9) (Anderson, 1996; Hough et al., 1997). The GuKc domain is rendered inactive and does not confer kinase activity, the PDZ domain is well known to interact with numerous transmembrane proteins (Kornau et al., 1995).

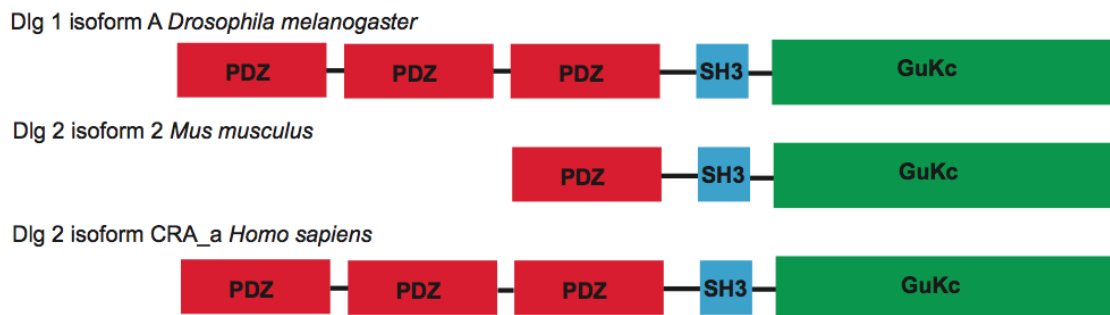


**Figure 9** Dlg1 homologs in *Drosophila melanogaster*, *Mus musculus* and *Homo sapiens*

Dlg1 isoform A in *Drosophila* has 3 PDZ domains, followed by the SH3 domain and the GuKc domain. The Dlg2 isoform CRA\_a of *Homo sapiens* shows the same structure whereas Dlg2 isoform 2 of *Mus musculus* only displays one PDZ domain.

Dlg1 is conserved up to humans which have four different Dlg homologs: Dlg1 (hDlg/SAP97), Dlg2 (PSD-93/ Chapsyn-110), Dlg3 (NE-Dlg/SAP102) and Dlg4 (PSD-95/ SAP90) (Cho et al., 1992; Lue et al., 1994; Brenman et al., 1996; Makino et al., 1997; Hanada et al., 2000). Similar to *Drosophila Dlg1*, the vertebrate homologs were found to be involved in epithelial polarity, tumor suppression, and functional morphology of the postsynaptic density.

When the rat proteins Dlg1/SAP97 and Dlg3/SAP102 were heterologously expressed in *Drosophila Dlg1* mutants, they were able to rescue synaptic bouton structure and suppress tumor formation (Thomas et al., 1997). This demonstrates how closely related mammalian and *Drosophila* Dlg proteins are, not only on a structural but also on a functional level.

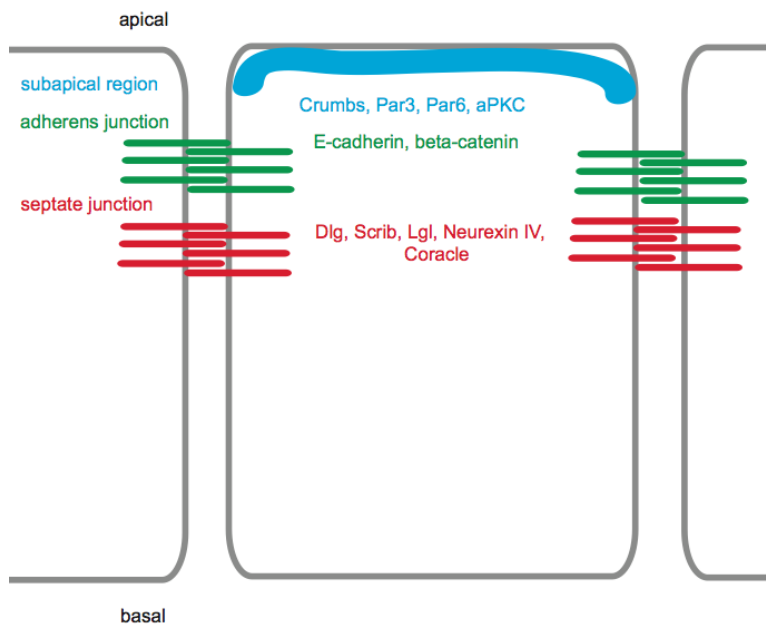


**Figure 10 Junctional complexes involved in *Drosophila* epithelial polarity**

In the subapical region of epithelial cells, Crumbs, Par3, Par6 and aPKC are expressed (blue). The adherens junction (green) is located basally to the subapical region, bearing the proteins E-cadherin and  $\beta$ -catenin. Basolaterally, *Drosophila* possesses a septate junction (red). In this region of the cell, Dlg, Scrib, Lgl, Neurexin IV, and Coracle are located. (modified from Humbert et al., 2003)

### **2.6.2 Dlg1 establishes polarity in *Drosophila* epithelia**

Dlg1 localizes basolaterally and is concentrated at septate junctions in *Drosophila* epithelia where it builds a complex together with Scribbled (Scrib) and Lethal (2) giant larvae (Lgl) to separate the apical from the basolateral membrane domain (Woods and Bryant, 1991; Bilder et al., 2002).

Septate junctions are the homologs of vertebrate tight junctions (Bryant, 1996). Apically of the septate junction, the adherens junction mediates cell-to-cell connection and forms an adhering belt which runs all around the cell, which is also known as the zonula adherens (Fig. 10) (Bilder et al., 2002). In *Drosophila*, the subapical region concentrates proteins like Crumbs, Par3, Par6 and aPKC, all of which are important for epithelial polarity (Fig. 10) (Petronczki and Knoblich, 2000; Wodarz et al., 2000). Interestingly, Scrib helps to localize these apical determinants and when Scrib is knocked-down, these proteins together with the adherens junction move to the basolateral part of the cell (Bilder and Perrimon, 2000). However, the localization of basolateral determinants like Dlg1 remains unchanged (Bilder and Perrimon, 2000). This compartmentalization of the cell helps to form its overall shape and specify an internal morphological and signaling structure (Anderson, 1996). For example, Dlg1 was shown in humans to bind to the actin cytoskeleton via 4.1 proteins (Lue et al., 1994). Human Dlg1 is recruited to the sites of cell-cell-adhesion by E-cadherin, a component of adherens junctions (Reuver and Garner, 1998).

Hough and colleagues showed in 1997 that the HOOK domain of Dlg1 is required for Dlg1 localization to the cell membrane whereas without its second PDZ domain, the protein is mislocalized away from septate junctions. Additionally, PDZ 2 and 3 are important for epithelial growth regulation whereas SH3 and HOOK are involved both in epithelial polarity and growth control.

### **2.6.3 Dlg1 is a tumor suppressor**

The essential role Dlg1 plays for proper morphology of epithelia already implies that loss of *Dlg1* expression might lead to cell proliferation, tissue growth and tumor formation. Indeed, a loss-of-function *Dlg1* mutation leads to a disruption of septate junctions and as a consequence to neoplastic imaginal disc overgrowth, hence the name of the gene (Woods et al., 1996; Woods et al., 1997; Woodhouse et al., 1998). Furthermore, when

embryos with temperature-sensitive *Dlg1* alleles were temperature-shifted such that Dlg1 function was lost, follicle cells of the *Drosophila* egg chamber leave the mono-layered follicular epithelium which ensheathes the germ cells, lose their polarized, cube-like cell shape and invade into the germ cell area (Goode and Perrimon, 1997). This was another clear evidence that Dlg1 is not only passively involved in cell polarization and cell adhesion but that its loss can also induce neoplasia which resembles tumor growth and metastatic behavior of cells.

Consequently, Dlg1 in humans is mainly expressed in non-proliferative cell types, e.g. differentiated epithelia, neurons, muscle tissue including the heart, and cells of the Langerhans Islets in the pancreas (Makino et al., 1997). To the contrary, little Dlg expression was detected in cancer cell lines (Makino et al., 1997). When Dlg was overexpressed in cancer cell lines, suppression of growth could be detected (Hanada et al., 2000)

#### **2.6.4 Dlg1's role in neurons**

Dlg1 is required for the formation of proper synaptic junctions in the *Drosophila* neuronal system (Budnik et al., 1996). In addition to inter-neuronal synapses, the synaptic connections between motor neurons and muscles also require Dlg1. *Dlg1* knock-out results in larger postsynaptic currents at the neuromuscular junction (Budnik et al., 1996). A later study could show that the HOOK domain which is the region between the SH3 and GuKc domain recruits Dlg1 to the postsynaptic membrane (Thomas et al., 2000). Furthermore, large membraneous clusters of Dlg1 appeared when PDZ domains 1 and 2 were deleted. Finally, the GuKc domain seems to control Dlg1 trafficking between the cell compartments (Thomas et al., 2000).

In *Drosophila*, Dlg1 helps the localization of the Shaker potassium channel as well as the localization of the cell adhesion molecule Fasciclin II to the synaptic membrane (Zito et al., 1997).

In mammalian neurons, Dlg4/PSD-95 interacts with the cytoplasmic tail of the NMDA receptor (Kornau et al., 1995) and if knocked down, this causes enhanced long term potentiation defects leading to a severely impaired spatial learning process (Migaud et al., 1998). Mechanistically, Dlg2/PSD-93 and Dlg4/PSD-95 bind to the NMDA receptor and the enzyme neuronal nitric oxide synthase (Brenman et al., 1996). Thereby,

calcium influx through the NMDA receptor can be coupled to the enzyme's activity. Thus, Dlg1 is required for learning processes in the central nervous system.

### **2.6.5 Dlg1's role in muscle**

The function of Dlg1 in neither muscle nor heart is well investigated. A *Dlg1* knock-out in mice displays severe defects with urinary tract development, including a reorientation of the circular smooth muscles around the ureter into a longitudinal orientation (Mahoney et al., 2006). This suggests a potential function for Dlg1 in smooth muscle orientation in the mouse ureter. In *Drosophila*, *Dlg1* knock-down in all muscles leads to lethality, however, the molecular cause for this lethality has not been investigated (Schnorrer et al., 2010).

## **2.7 The method of RNA interference (RNAi)**

The first hints, that the introduction of RNA into a host cell might induce interference with host mRNA came from a study in 1984, when Izant and Weintraub transfected mouse L cells with a construct that contained an antisense Herpes simplex virus (HSV) thymidine kinase (TK) gene. When they coinjected the antisense DNA with wild type TK DNA at a ratio of 100:1 into TK- L cells, they were able to detect a reduction of HSV TK gene expression (Izant and Weintraub, 1984).

Later on, *C. elegans* served as the model system of choice to further investigate this mechanism of RNA-induced gene silencing. Soon, it was clear that exogenous double-stranded RNA of a length of 26-81bp (Parrish et al., 2000) was much more effective in gene silencing than single-stranded RNA (Fire et al., 1998). It was concluded that the single strands must be subject to internal degradation mechanisms and therefore could not be involved in silencing of the target genes. After injection of the long RNA duplex, Parrish and colleagues detected processing of the long RNA into smaller, about 25 nucleotide long pieces suggesting a mechanism how those exogenous RNA molecules may function in the organism.

RNA interference was shown to be cell non-autonomous in *C. elegans* thereby rendering tissue-specific gene silencing impossible (Fire et al., 1998). However, in *Drosophila*, RNA interference is cell autonomous (Roignant, 2003). Thus, it can be used to achieve tissue-specific gene knock-down.

When a double-stranded exogenous RNA enters a *Drosophila* cell, it is cleaved into 21- to 23-nucleotide long small interfering (si) RNA by the RNase III enzyme Dicer2 (Zamore et al., 2000; Bernstein et al., 2001). These siRNAs are transported by R2D2 to the nuclease complex RNA-initiated silencing complex (RISC) (Liu, 2003) and serve as templates to guide sequence-specific mRNA degradation (Hammond, 2001).

The perspective of tissue-specific RNAi in an intact organism was the motivation for the construction of genome-wide RNAi libraries in *Drosophila*. The construction of an RNAi library which covers 88% of the predicted protein-coding genes in *Drosophila* was reported (Dietzl et al., 2007). The library uses the GAL4/ UAS system. The inverted repeats are cloned into a UAS vector and result in the tissue-specific formation of siRNAs when crossed to a GAL4 line of interest (Brand and Perrimon, 1993). Thus, tissue-specific expression of the hairpin is possible by combining it with a tissue-specific driver coupled to the GAL4 construct. Additionally, an alternative library of short hairpin (sh) RNA constructs was built which mediates strong gene silencing during oogenesis (Ni et al., 2011).

The genome-wide RNAi library was successfully tested in the muscle system of *Drosophila*. A genome-wide screen identified a role for more than 2,000 genes in muscle, many of which have some function in myofibril or sarcomere morphogenesis (Schnorrer et al., 2010).

This muscle-specific screen also builds the basis for the research project presented in this thesis. Some of the identified genes were selected for further investigation in the heart, among them also *Dlg1*.

## **2.8 Genomic GFP-tagged fosmid clones in the adult *Drosophila* heart**

To further characterize adult heart morphology, we investigated the localization of a selected number of GFP-tagged proteins (Ejsmont et al., 2009; Sarov et al., unpublished). Fosmid vectors carry *Drosophila* genomic DNA fragments up to 40kb in size. Thus, the genes from this library keep their native genomic context and can be recombineered in bacteria to add a GFP tag to a gene of interest. After tagging, the fosmid is integrated into

the fly genome site-specifically and gene expression can be determined (Ejsmont et al., 2009).

A disadvantage in the application of P-elements is their random integration into the genome. This is prevented by introducing an *attB* site into the fosmid construct. This site is recognized by the bacteriophage phiC31 integrase which then mediates the integration of the construct into the genome's *attP* site via homologous recombination (Groth et al., 2004). *attP* sites can be introduced into the genome. Generally, the three intrinsic *attP* sites in *Drosophila* are not used by phiC31 integrase which makes integration into the newly-introduced, artificial *attP* sites possible in a controlled manner (Groth et al., 2004; Bischof et al., 2007).

A fosmid vector library which contains GFP-tagged genes (Sarov et al., unpublished) is a valuable resource for the *Drosophila* community as the GFP-tagged proteins are under their endogenous promotor and thus should be fully functional. They can be used to determine protein localization, also in living specimen, and to purify protein complexes using standard IP-grade antibodies. As a quality control of the library, the fosmids have to be tested for their reliable expression in different tissues, e.g. the adult heart, first. The results of the cardiac tests are included in this thesis work.

## **2.9 Aim of this study**

The aim of this study was to identify factors important for myofibrillogenesis in the adult *Drosophila* heart as well as to elucidate their spatial and temporal functions in determination of cardiac myofibril arrangement. In detail, I wanted to address the question how myofibrils are arranged circularly around the heart lumen. Furthermore, I wanted to find out how and where the myofibrils are anchored in order to reach their correct position within the cell. This correct orientation is essential for proper function of the heart.

In order to reach this aim, I used the RNA interference methodology. *Discs large 1* was selected as a candidate gene due to its interesting myofibril misarrangement phenotype when knocked-down by RNAi.

### 3. Results

#### 3.1 Time course of adult cardiac myofibrillogenesis

Without coordinated contraction of the myofibrils, heartbeat would not be possible. Thus, the correct morphogenesis of cardiac myofibrils is essential for proper function of the heart. Although many studies have described cardiac myofibrillogenesis in the chick heart (for example Du et al., 2008), a detailed description of myofibrillogenesis at different stages of *Drosophila* cardiac development was still missing. Therefore, I investigated myofibrillogenesis of the developing adult heart during larval and pupal stages (Fig.11). To visualize the adult heart in wild type, I dissected hearts at the third larval instar stage, and visualized the myofibrils by phalloidin staining. I detected myofibrils that circularly run around the heart tube (Fig. 11 A, A'), and are relatively regularly spaced but not densely packed or highly ordered yet. When the fly starts cardiac remodeling during metamorphosis, the larval myofibrils are degraded and thus absent from about 24h after puparium formation (APF) (data not shown). New fibrils are built up during pupal myofibrillogenesis. The first signs of punctate actin condensation can be detected around 46h APF (Fig. 11 B, B'). These actin condensations are already arranged in lines which determine the pattern of the mature myofibrils. At 54h APF, many distinct myofibrils are present, all of which orient in a circular pattern around the heart lumen (Fig. 11 C, C'). Until the end of pupal development, the density of the myofibrils increases further and the myofibrils become thicker, resulting in densely packed myofibrils in adult cardiomyocytes (Fig. 11 D, D'). In summary, myofibrils are degraded at the third larval instar and are slowly built up again via actin condensations serving as the starting point for mature myofibrils that fill up the entire cardiomyocyte.

Next, I sought to take a closer look at the overall heart morphology at both the L3 and adult stages (Fig. 12). I wanted to determine where the myofibrils were located within the cardiomyocytes in relation to the luminal and abluminal cell membranes, as well as the nuclei. To this end, I stained the cell membrane with an antibody against the cell cortex protein  $\alpha$ -spectrin (Fig. 12 A, B). However in the larval heart,  $\alpha$ -spectrin staining seems to be more confined to the myofibrils than to the cell membrane (Fig. 12

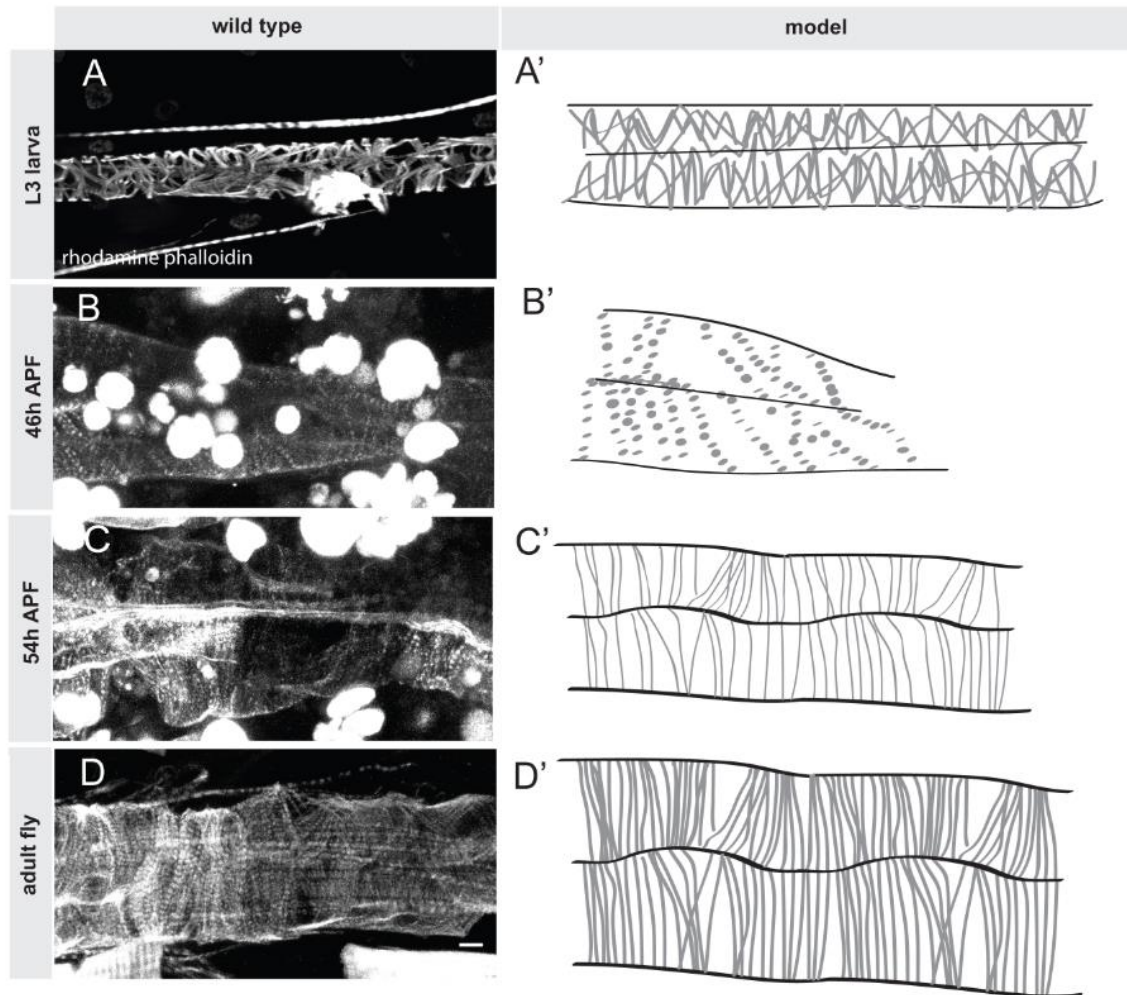


**Figure 11 Developmental time course of adult cardiac myofibrillogenesis**

(A-D) Dissected hearts of *UAS-dcr2,w-;HandGAL4* flies (further referred to as wild type genotype) L3 larval stage (A), 46h APF (B), 54h APF (C) and adult stage (D). Myofibrils were stained with rhodamine phalloidin. Models depicting myofibrils at the respective time points are shown (A'-D'). Note the formation of highly dense, regularly oriented myofibrils from 46h APF to adult stage. Scale bar: 100 $\mu$ m

A). Larval myofibrils do not yet show the high order of parallel packaging (Fig. 12 A'') as can be found in the adult. In the adult, myofibrils build a thin layer (Fig. 12 B'') which is located closer to the outer cell membrane than to the inner one. The nuclei are located between the fibrils and the lumen and cause the luminal cell membrane to form distinct bulges which extend into the heart lumen (Fig. 12 B, B' arrows). In the adult, nuclei usually form pairs, meaning each nucleus of one cardiomyocyte row is located directly opposite to the one of the other cell row (boxes in Fig. 12 B'). In the larva, nuclear position is not that highly ordered yet (Fig. 12 A').

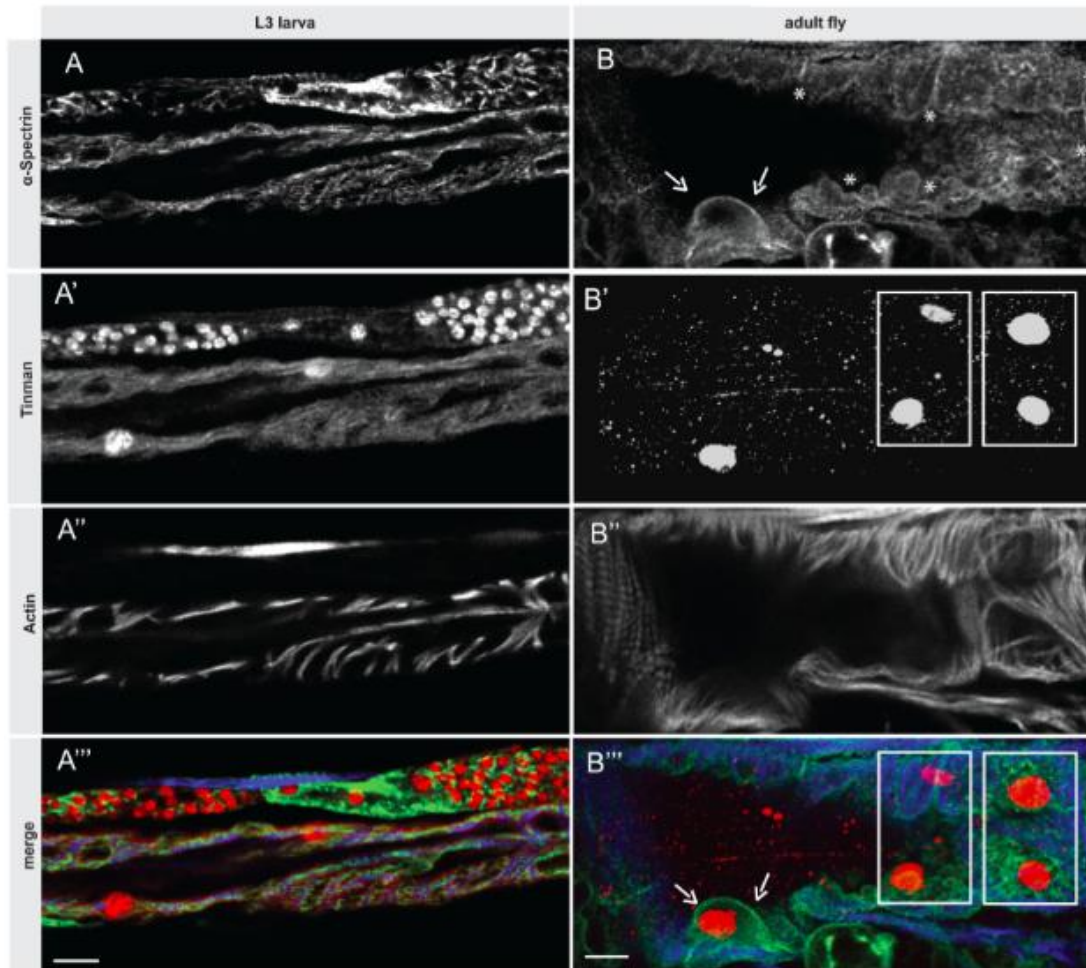


**Figure 12 Heart morphology in L3 larvae and adult flies**

Optical section through an L3 larval heart (A-A''') and an adult heart (B-B''') of wild type flies stained for cardiac nuclei (Tinman, red), the cell-cortex protein  $\alpha$ -spectrin (green) and actin (phalloidin-Alexa660, shown in blue). The arrows point out the cell body extending into the cardiac lumen. The boxes show how two nuclei of the opposing rows are arranged in pairs. The third pair does exist but is not shown due to localization in a different Z-plane. The asterisks in B show parts of the transverse cell-cell junction. Scale bars: 100 $\mu$ m

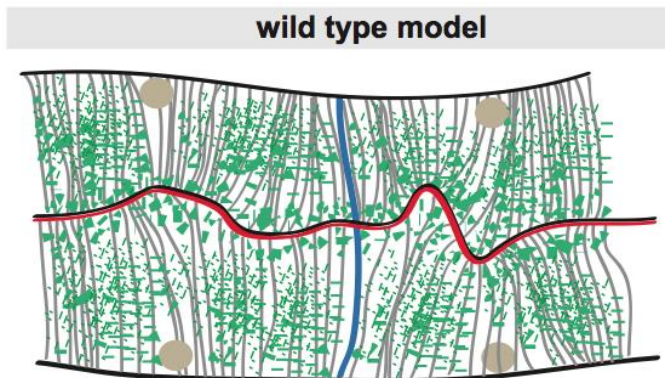
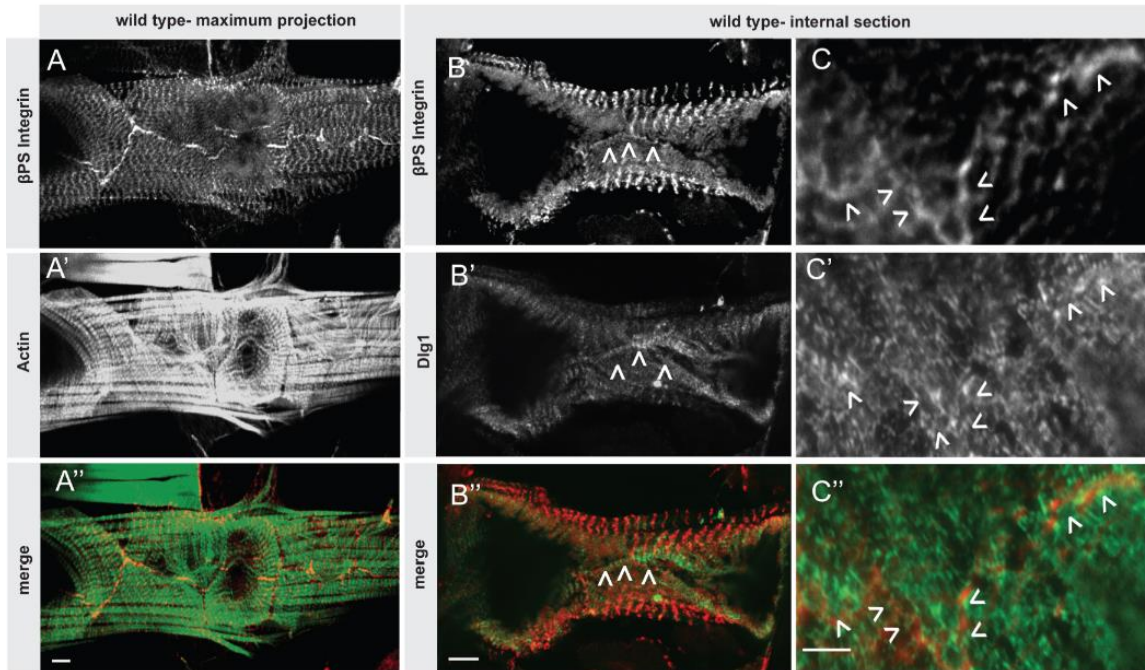


**Figure 13  $\beta$ PS integrin and Dlg1 localization in the adult heart**

Wild type adult heart stained for  $\beta$ PS integrin (A, B, C, red), actin (A', green), and Dlg1 (B', C', green) is shown.  $\beta$ PS integrin is located at the longitudinal cell-cell junction extending from anterior to posterior along the heart tube as shown in this maximum projection of the ventral part of the heart (A). As can be seen in A'', myofibrils stand in a 90° angle on the longitudinal  $\beta$ PS integrin pool. This is also shown in a model of the ventral side of the heart looked upon from the lumen, in which the cell membrane is black, the longitudinal  $\beta$ PS integrin pool is red, Dlg1 is green, the nuclei are brown and the transverse cell-cell junction is marked in blue. The longitudinal fibrils showing in A' do not belong to the heart, but are somatic muscle fibers that run beneath the adult heart.

Adult flies of the *Dlg1-GFP* line are stained for  $\beta$ PS integrin (B, C) and GFP (B', C') to show that Dlg1 is concentrated around the longitudinal  $\beta$ PS integrin pool (B', C' and arrowheads). Scale bar (A- A''): 100 $\mu$ m, scale bars (B- B'' and C- C''): 40  $\mu$ m

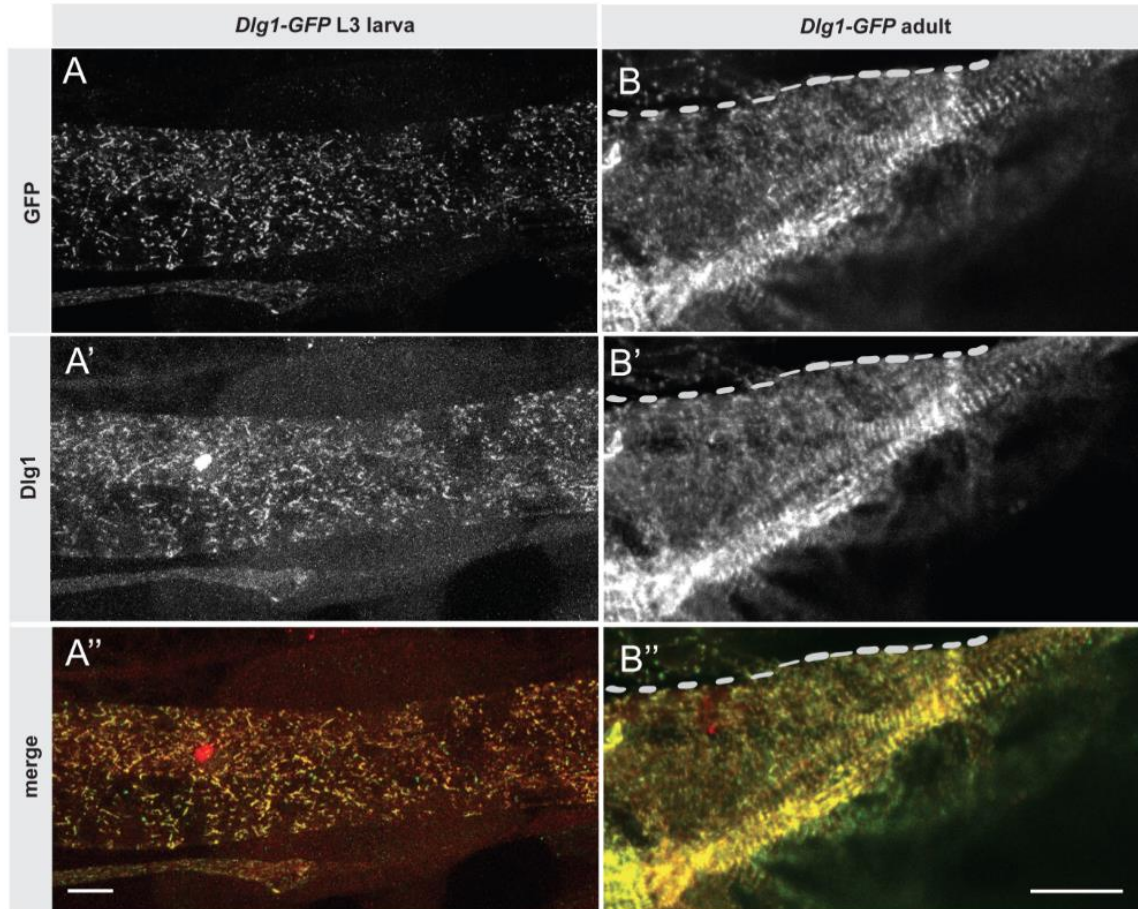


**Fig. 14 The *Dlg1-GFP* trap line signal overlaps with the Dlg1 antibody staining**

The *Dlg1-GFP* trap line was dissected at the larval L3 (A-A'') and adult stage (B-B'') and stained for GFP (A, B, green) and Dlg1 (A', B', red). Both stainings almost completely overlap and thus, the *Dlg1-GFP* fly line can be used equally to the Dlg1 antibody staining. Scale bars: 100 $\mu$ m

### 3.2 Localization of junctional proteins in larval and adult hearts

#### 3.2.1 Integrin localizes differentially to the longitudinal cell-cell junction

In muscle, myofibrils are anchored at integrin containing cell-matrix adhesion sites. To visualize integrin localization in adult heart, I stained hearts with anti- $\beta$ PS integrin. Interestingly, in the wild type,  $\beta$ PS integrin is mainly concentrated at the longitudinal cell-cell junction which runs from anterior to posterior along the heart (Fig. 13 A). In most cases, myofibrils are anchored at this junction and oriented in a right angle to these cell contacts (Fig. 13 A', A'').

Together, this indicates a possible polarity in the adult heart, as integrins preferentially concentrate at the longitudinal cell-cell contacts at which the circular

myofibrils surrounding the heart lumen originate. In order to identify candidate genes that determine the polar organization of adult cardiomyocytes with a defined orientation of their circular myofibrils, that are anchored to the ECM and to the longitudinal cell-cell junction, we decided to investigate proteins with a well defined role in epithelial polarity.

The epithelial polarity protein Dlg1 is well known for its crucial role in establishing the basolateral membrane domain in *Drosophila* epithelia where it localizes to the basolateral membrane domain (Bilder et al., 2002). As it gives spatial identity to this membrane domain in epithelial cells, I was wondering if it might also play a role in establishing the typical morphology of the *Drosophila* cardiomyocyte.

To determine the localization of the polarity protein Dlg1 in the developing heart, I either used an anti-Dlg1 antibody or a *Dlg1-GFP* trap line which houses a GFP insertion within the endogenous *Dlg1* gene, thus creating a Dlg1-GFP fusion protein that is fully functional. Figures 14 A'' and B'' show, that the GFP signal of the *Dlg1-GFP* line completely overlaps with the Dlg1 antibody staining, therefore the *Dlg1-GFP* line can be used as an equivalent alternative to stainings with the Dlg1 antibody.

A concentration of Dlg1 surrounding the longitudinal  $\beta$ PS integrin pool was found (arrowheads in Fig. 13 B', C'). In addition, Dlg1 is found in a network pattern throughout the cardiomyocytes. I suggest that Dlg1 might help  $\beta$ PS integrin to localize at the longitudinal cell-cell junction and by that, to arrange the myofibrils in parallel around the heart tube.

Because the myofibrils are located just underneath the outer cell membrane, I was wondering if they are firmly attached to the membrane and to the surrounding ECM and how this attachment is mediated. Various studies in the somatic musculature both in *Drosophila* and vertebrates defined the costamere as the attachment complex between ECM, membrane and myofibril (Volk et al., 1990). Integrins are the most important markers for costameres. Therefore, I stained larval and adult hearts for the *Drosophila*  $\beta$ PS integrin (Fig. 15 A, B) and actin (Fig. 15 A', B') and found that  $\beta$ PS integrin

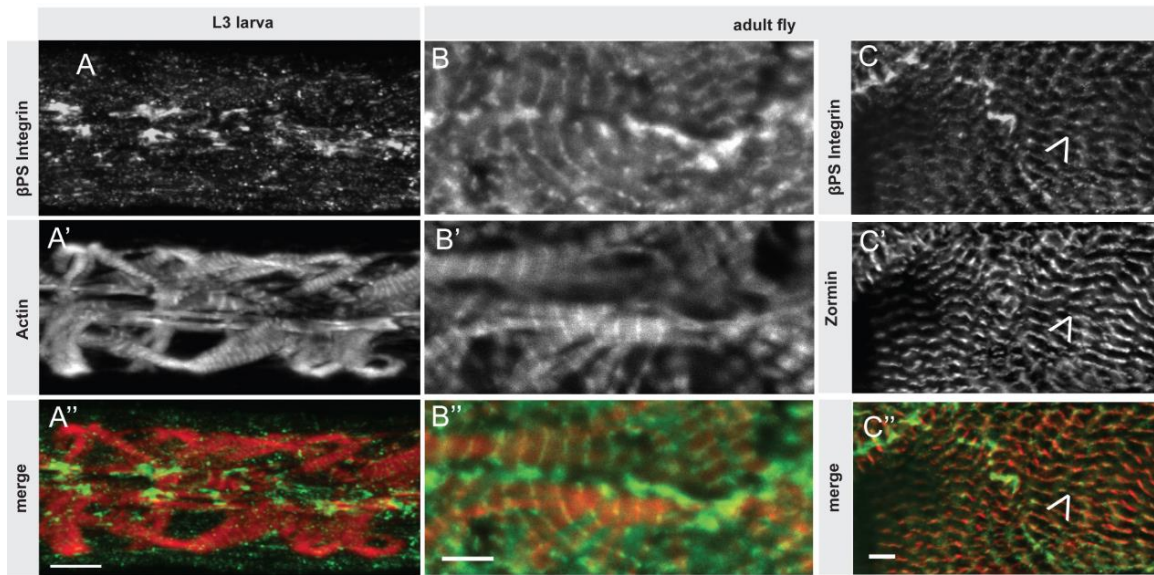


**Figure 15  $\beta$ PS integrin localizes along the myofibrils of the adult and larval heart**

Heart of the *Dlg1-GFP* trap line at larval L3 (A-A'') and adult (B-B'') stages stained for  $\beta$ PS integrin (A and B, green) and actin (A' and B', phalloidin-Alexa660 shown in red). Z-discs are stained with anti-zormin antibody (C', red) and costameres with the anti- $\beta$ PS integrin antibody (C, green). The arrowhead points towards an example of overlapping zormin and  $\beta$ PS integrin stainings at a costamere. Scale bars: 40 $\mu$ m

colocalizes with sarcomeric structures in a striated pattern in adult cardiomyocytes. To identify with which sarcomeric structure the integrin pattern associates, I costained adult hearts for  $\beta$ PS integrin and zormin, a Z-disc marker (Burkart et al., 2007). I found, that  $\beta$ PS integrin indeed localizes at the Z-discs (arrowhead in Fig. 15 C-C''). This shows, that in the adult *Drosophila* heart, integrins which are localized at the membrane and link to the ECM, couple intracellularly to actin at the costameric Z-disc and anchor the myofibrils to the membrane. Interestingly, such a tight connection of the myofibrils to the membrane appears absent in larval hearts and thus needs to be developed during pupal stages. In larva,  $\beta$ PS integrin is found at the ends of the myofibrils (Fig. 15 A'').

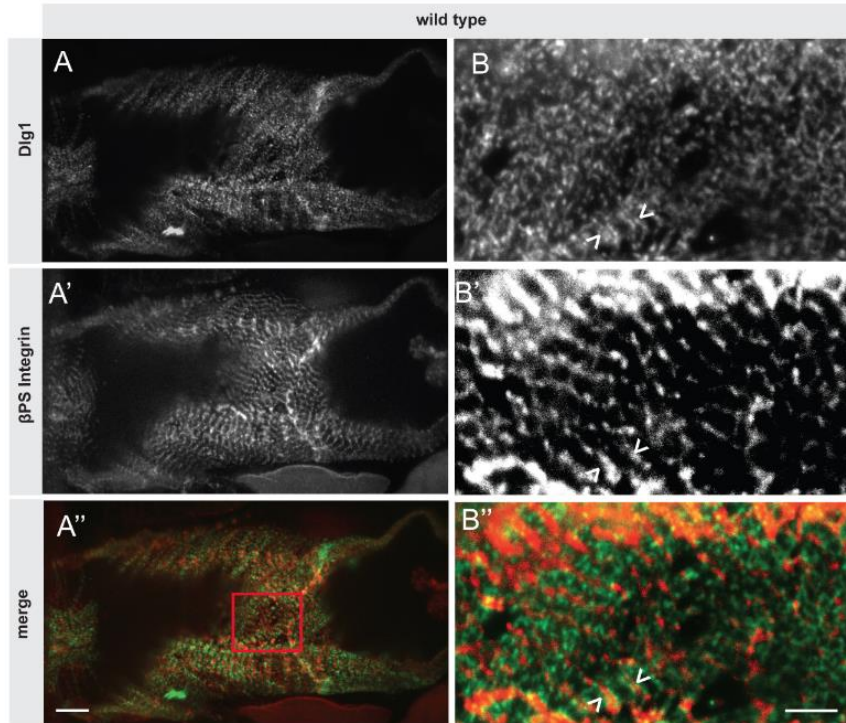


**Figure 16 Dlg1 is located closely to the costamere in adult**

Dlg1 is shown in green (A, B) and  $\beta$ PS integrin in red (A', B'), with B-B'' being a zoom in of the area in the red box (A''). The arrowhead points to an example of Dlg1 and  $\beta$ PS integrin staining located in distinct but closely associated spots. Scale bar (A-A''): 100 $\mu$ m, scale bar (B-B''): 40 $\mu$ m

### 3.2.2 Localization of the polarity protein Dlg1 in the *Drosophila* heart

First, I wanted to define the subcellular localization of the epithelial polarity protein Dlg1 in the cardiomyocyte in more detail and asked the question if Dlg1 might colocalize with the costameres. Therefore, I stained adult flies of the *Dlg1-GFP* trap line with  $\beta$ PS integrin antibody (Fig. 16 A', B') and found, that although Dlg1 does not show the same pattern as  $\beta$ PS integrin, the punctate patterns are closely associated (Fig. 16 B, B', B'' arrowheads), suggesting that Dlg1 may also somehow associate with myofibrils.

Next, I tested whether Dlg1 was expressed in the *Drosophila* heart during larval and pupal stages of development and where it is located in the cardiomyocytes (Fig. 17 A- C). Interestingly, at L3 and adult stages, Dlg1 is located closely to the myofibrils in a network-like pattern (Fig. 17 A, A' and D, D'). During metamorphosis, when adult myofibrils are built up, Dlg1 first appears in spacious plaques at 46h APF (Fig. 17 B') and is not yet distributed along the actin condensations which later on will form the

myofibrils. At 54h APF (Fig. 17 C'), Dlg1 appears in a dotted pattern, already starting to build the network-like structure that can be found in the adult. From these experiments I can conclude, that Dlg1 is expressed at all stages of cardiac development and associates with myofibrils at least in larval and adult cardiomyocytes.

To further characterize Dlg1 localization within the cell, I compared Dlg1 localization with the sarcomeric Z-disc protein zormin (Fig. 18). Again, stainings were performed in the *Dlg1-GFP* trap line. In several cases, a close but distinct location between Dlg1 and zormin was detected (arrowheads Fig. 18 A- A''). Thus, the Dlg1 network is associated with the zormin staining and might therefore be in close contact

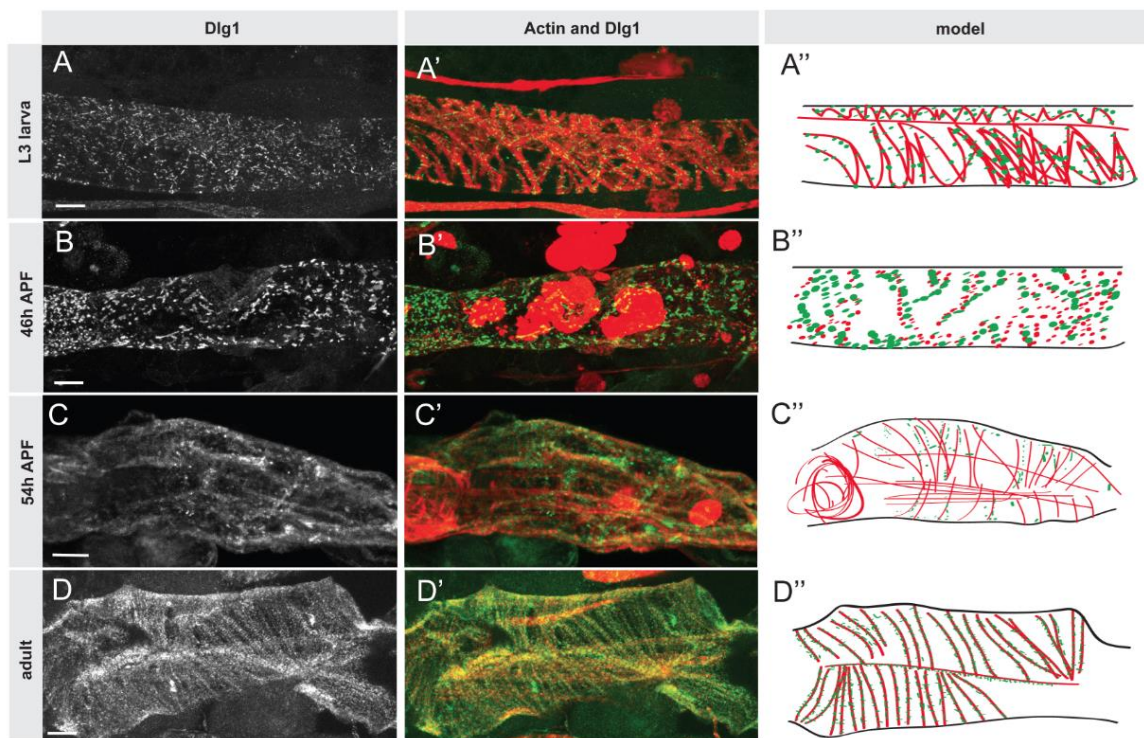


**Figure 17 Developmental distribution of Dlg1 during myofibril formation**

The *Dlg1-GFP* trap line at the larval L3 (A-A'') stage, 46h APF (B-B''), 54h APF (C-C'') and the adult stage (D-D''). Dlg1 was stained for with an anti-GFP antibody (A-D, green) and actin with phalloidin (red, A'-D'). Models are depicted in A''-D'' where Dlg1 is shown in green and myofibrils in red. Scale bars: 100µm

with the sarcomere. As Dlg1 does not colocalize with a sarcomeric component I stained for the sarcoplasmic reticulum calcium ATPase SERCA (Fig. 18 B- B''). I found a different punctate pattern for SERCA which again sometimes shows a close association

with Dlg1 (arrowheads). It is therefore reasonable to conclude, that Dlg1 is not located at the sarcoplasmic reticulum but at a structure close to it.

I wanted to identify the subcellular compartment at which Dlg1 is really located in the cardiomyocyte. Also, it had been published, that Dlg1 partly colocalizes with amphiphysin, a marker for the T-tubular system, in *Drosophila* flight muscle (Razzaq, 2001). Therefore, I costained adult cardiomyocytes of an *amphiphysin-YFP* trap line with the antibody against Dlg1 (Fig. 19) and found a good degree of overlap (Fig. 19 B''), arrowheads). This overlap is also shown in plot profiles which were drawn from the area indicated by the white line. Peaks 1-6 appear in the plots from both the Dlg1 and the

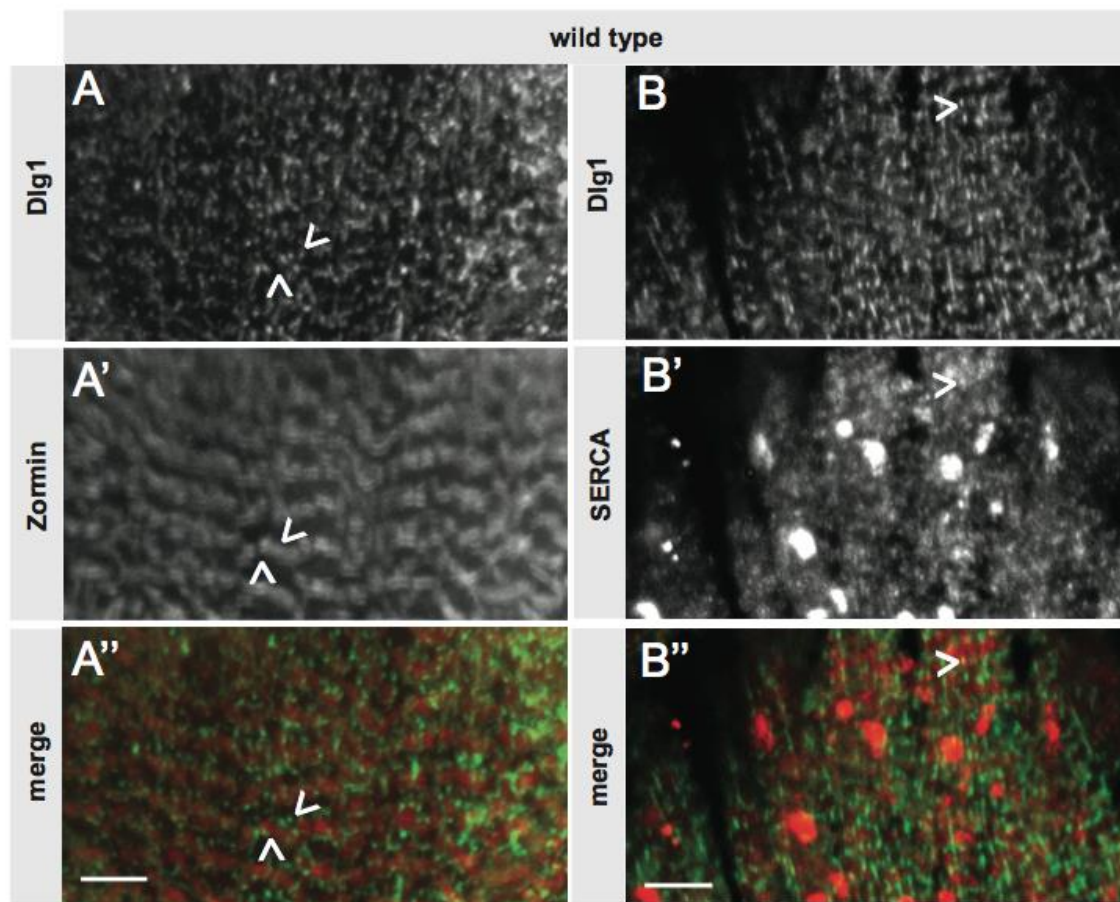


**Figure 18 Dlg1 is located adjacent to the sarcomeric Z-disc and the sarcoplasmic reticulum in adult heart**

Staining of Dlg1 (green, A) and zormin (red, A') in a wild type adult heart. Arrowheads point out examples where there is a close association of the two proteins. The sarcoplasmic reticulum calcium ATPase SERCA is stained in red (B') and Dlg1 in green (B) in a wild type adult heart. Arrowheads point out where there is a close association of the two proteins. Scale bars: 40µm

amphiphysin channel suggesting that Dlg1 is indeed localized at the T-tubular membrane system.

This amphiphysin-dominated membrane domain is found in vicinity to the myofibrils (cross section in Fig. 20) in accordance with it being a marker for the T-tubular system which reaches from the membrane surface far down to the myofibrils (Lehmacher et al., 2012). In contrast,  $\alpha$ -spectrin marks the cell cortex (Fig. 20 A and 21 A', B') and Dlg1 does neither overlap in a sagittal (Fig. 21 A) nor in a cross section (Fig. 21 B). This, too, confirms our hypothesis that Dlg1 is associated with the membranous T-tubular system and might therefore represent an important link between membrane and myofibril.

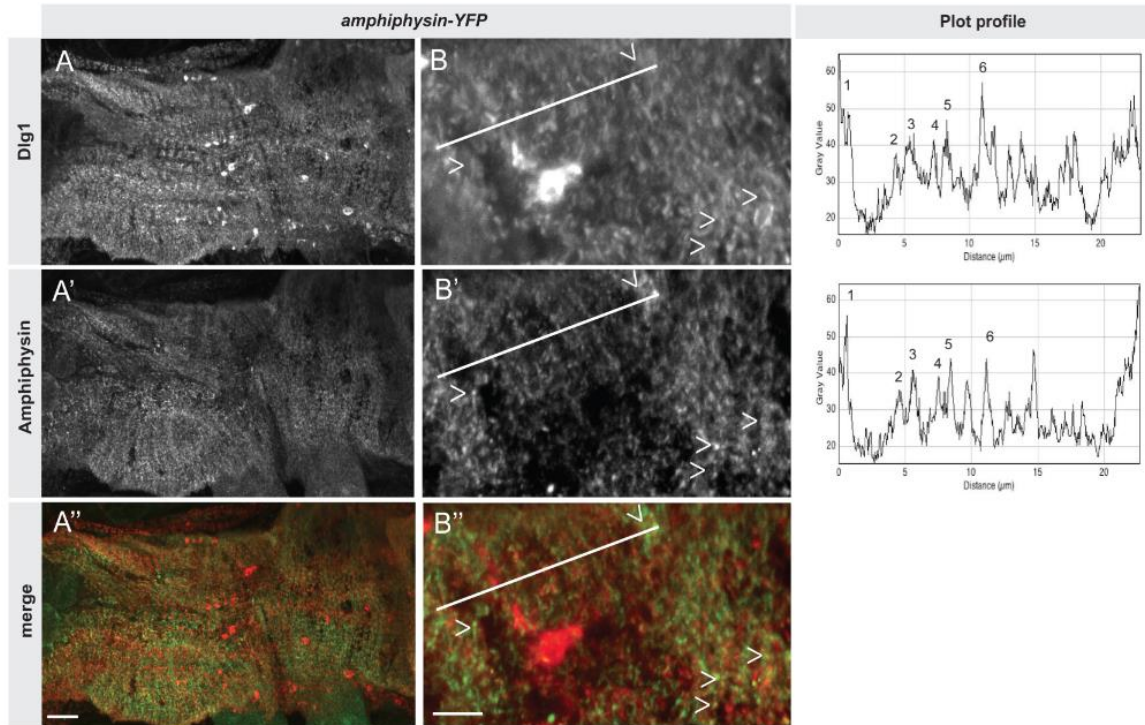


**Figure 19 Dlg1 localizes to T-tubules in the adult heart**

An *amphiphysin-YFP* line was dissected at the adult stage and stained for Dlg1 (A, B, red) and GFP (A', B', green). Plot profiles of the respective channels are shown on the right and peaks existent in both channels are numbered. A white line shows where the plot profile was made. Additionally, arrowheads point to examples of overlapping expression. Scale bar (A- A''): 100µm, scale bar (B- B''): 40µm

### 3.3 The role of Dlg1 in heart

#### 3.3.1 The adult *Dlg1* loss-of-function phenotype

To functionally investigate the role of Dlg1 in the heart, I knocked down *Dlg1*, making use of a transgenic RNAi line *UAS-Dlg1-IR* (#41134) from the Vienna Drosophila RNAi Center (Fig. 22). This resulted in a remarkable phenotype, namely a chaotic misarrangement of cardiac myofibrils (Fig. 22 B'') and a changed heartbeat direction with the heart now beating in the anterior-posterior direction instead of the dorsal-ventral one (data not shown). Myofibrils mostly run longitudinally along the tube instead of circularly around it. The myofibrillar misarrangement is quantified in Figure 23 and images of the different misarrangement categories are displayed. Indeed, a profound myofibrillar misarrangement was found upon knock-down of *Dlg1* suggesting that Dlg1 is required for proper organization of the cardiac myofibrils. As Dlg1 in epithelia regulates cellular positioning within the epithelium, I wanted to test if the two opposing rows of cardiomyocytes are still arranged normally in *Dlg1* knock-down hearts. In wild type, the two cardiomyocytes that are attached to each other are located opposite

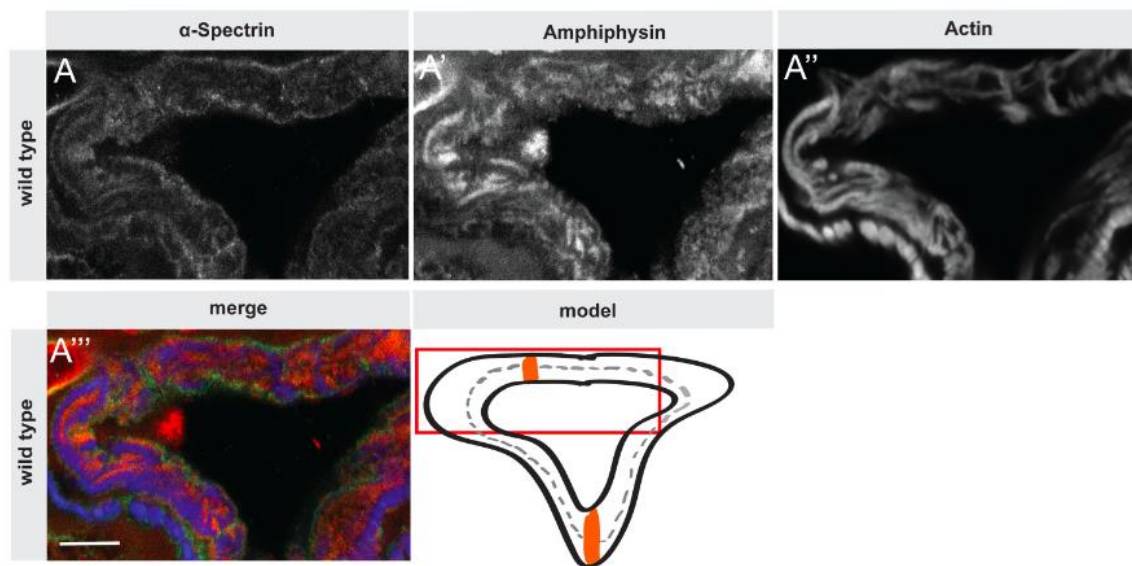


**Figure 20  $\alpha$ -Spectrin labels the cell cortex, whereas amphiphysin labeling can be detected in vicinity of the myofibrils**

Cross section of an adult wild type heart.  $\alpha$ -Spectrin (A, green), amphiphysin (A', red) and actin stainings (A'', blue) are shown. By these stainings, two different membrane domains, namely the cortical ( $\alpha$ -spectrin) and the T-tubular (amphiphysin) one, can be identified. Scale bar: 100 $\mu$ m

to each other to form a tube. I stained the nuclei in *Dlg1* knock-down hearts and showed that the position of the nuclei is largely unchanged (Fig. 23), suggesting that the nuclear positioning in the heart tube is preserved despite the major myofibrillar orientation phenotype.

Gene knock-down by RNAi can potentially have off-target effects (Ma et al., 2006; Dietzl et al., 2007). To verify knock-down specificity of *Dlg1*, I set up a rescue experiment in which I tried to rescue the knock-down of *Dlg1* by the 41134 RNAi line via co-overexpression of *Dlg1* with *UAS-Dlg1-GFP*.

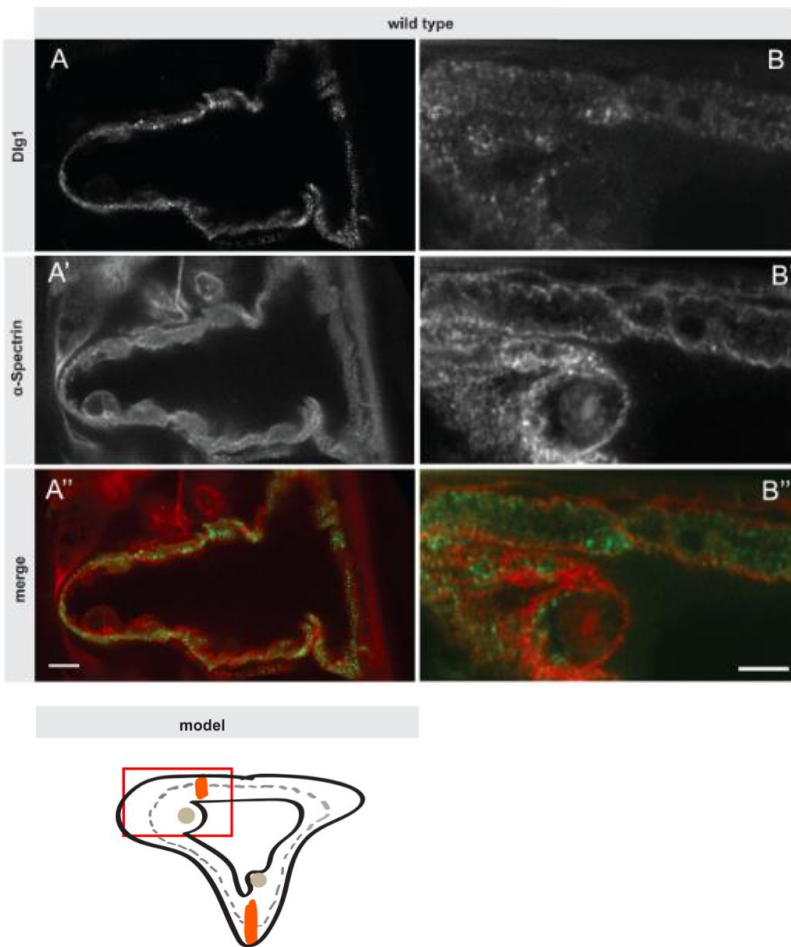


**Figure 21 *Dlg1* staining does not overlap with  $\alpha$ -spectrin staining in the adult heart**

Dissection (A) of the adult *Dlg1-GFP* trap line. B-B'' shows a cross section of which a model is shown. *Dlg1* (A, B, green) and  $\alpha$ -spectrin staining (A', B', red). Scale bar (A-A''): 100 $\mu$ m, scale bar (B-B''): 40 $\mu$ m

Unfortunately, myofibril arrangement was still chaotic and Dlg1-GFP could not be detected (Fig. 24), most likely due to the strong knock-down of the RNAi line. Thus, this experiment was not conclusive.

An alternative to demonstrate RNAi specificity is to use different independent hairpins to confirm the knock-down phenotype. Therefore, I tested additional RNAi lines from the Harvard Transgenic RNAi Project (TRiP). Out of eleven tested, three gave phenotypes that were similar or even more severe than the initial *UAS-Dlg1-IR 41134* one (Fig. 25 A', B'). In those three hairpin lines (two shown), *Dlg1* knock-down was even effective without overexpression of *UAS-dcr2* (Fig. 25 C'), which was shown to enhance RNAi efficiently, but also potential off-target effects (Dietzl et al., 2007). The TRiP lines are targeted to two different regions of the *Dlg1* mRNA which encode for PDZ domains 1 and 2 and thus, are different to the VDRC line (Fig. 26). The rescue of the TRiP RNAi lines gave the same result as with the 41134 RNAi line although it was done without *dcr2* (data not shown), again showing that even overexpressed Dlg1 is efficiently knocked-down.

However, because the knock-down with three TRiP lines resulted in a very similar phenotype as was seen with the VDRC line, I am convinced, that Dlg1 is required for proper circular arrangement of the myofibrils around the lumen of the heart. When Dlg1 is absent, myofibrils mainly orient longitudinally instead.

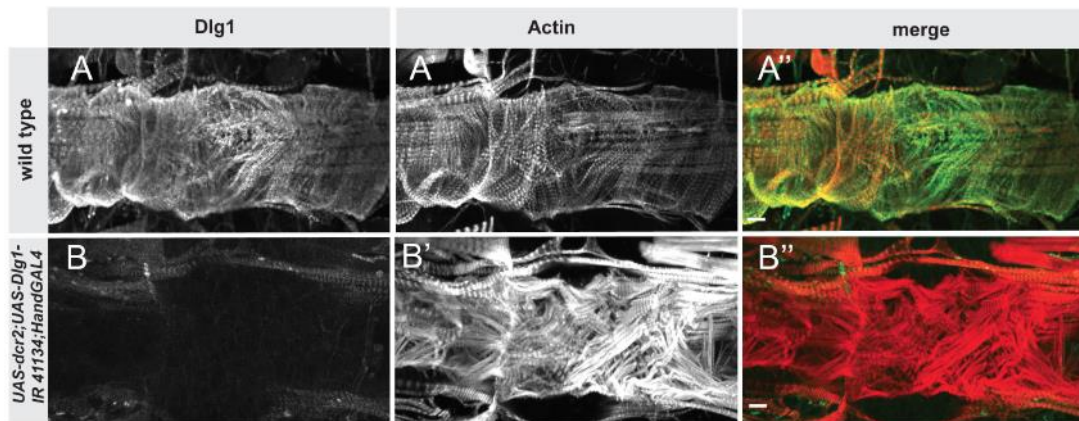


**Figure 22** *Dlg1* knock-down results in myofibril misarrangement

Adult wild type genotype and RNAi knock-down *UAS-dcr2;UAS-Dlg1-IR 41134;HandGAL4* stained for Dlg1 (A, B, green) and actin (A', B', red). Note the myofibrillar misarrangement upon *Dlg1* knock-down (B'') compared to the circular myofibrils in wild type (A''). Scale bars: 100 $\mu$ m

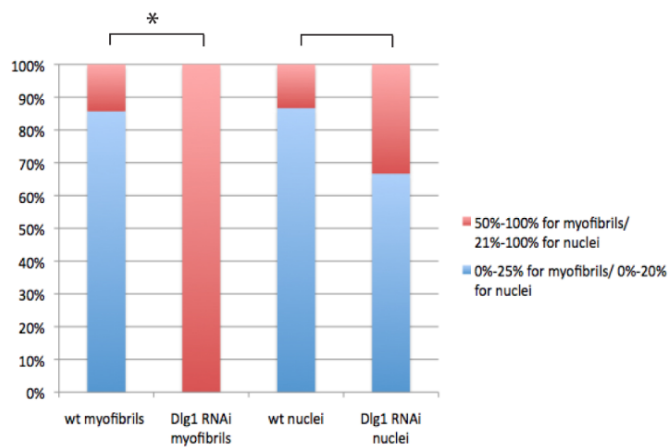
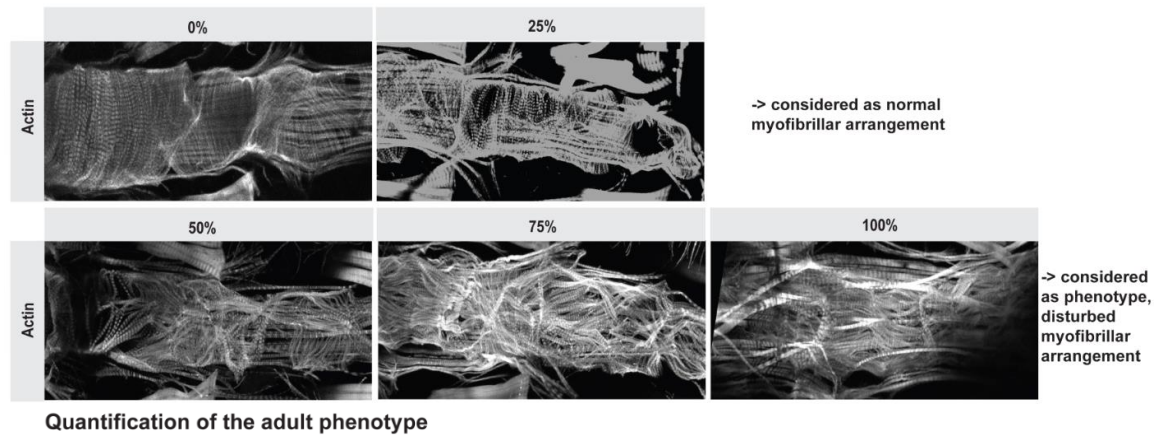


**Figure 23 Quantification of myofibrillar misarrangement and nuclear positioning upon *Dlg1* knock-down**

Phenotypic categories illustrate how which myofibrillar arrangement was quantified (0%, 25%, 50%, 75%, 100% misarrangement). In Materials and Methods, the quantification procedure for nuclear positioning is explained. Quantification results for adult wild type genotype and adult RNAi genotype are shown both for myofibrillar arrangement and nuclear positioning in the chart below. 0% to 25% myofibrillar misarrangement and 0% to 20% disturbed nuclear positioning are considered wild type, whereas 50% to 100% myofibrillar misarrangement and 21% to 100% disturbed nuclear positioning are considered a phenotype. Significance values were calculated using a one-tailed Fisher's Exact Test. Effects of *Dlg1* knock-down on myofibrillar arrangement are highly significant (which is indicated by an asterisk;  $p < 0.0001$ ), but not on nuclear position ( $p = 0.19$ ).

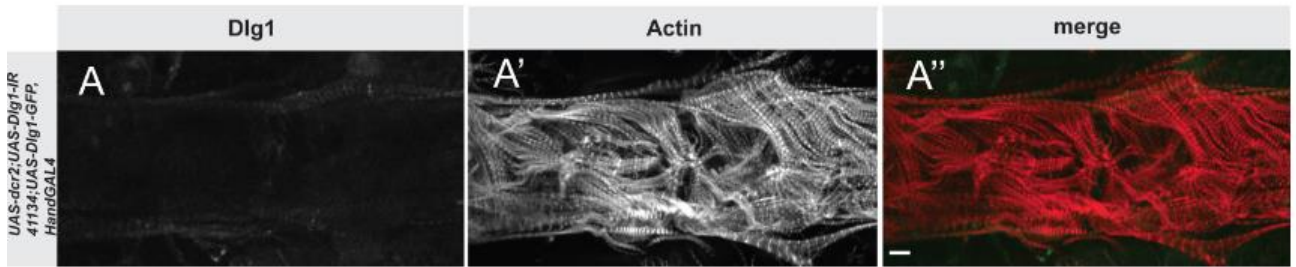


**Figure 24** *UAS-Dlg1-GFP* does not rescue the *Dlg1* knock-down

In the rescued adults *UAS-dcr2;UAS-Dlg1-IR 41134;UAS-Dlg1-GFP,HandGAL4* Dlg1 (A, green) is not expressed in the heart and myofibrillar arrangement is still chaotic (A'). Scale bar: 100µm

### 3.3.2 The *Dlg1* phenotype during development

Next, I wanted to find out when *Dlg1* is required for proper myofibril arrangement during heart morphogenesis. Therefore, I dissected L3 larval hearts and pupal hearts of the 41134 RNAi line, to be able to investigate time points before and during metamorphosis. At both time points, a severe myofibril misarrangement phenotype was detected (Fig. 27 A', B'), showing that Dlg1 is important for myofibrillar arrangement during larval and pupal stages of development. Again, nuclear positioning of the cardiomyocytes appeared largely unaffected (Fig. 27 D). Thus, we can conclude, that similar mechanisms are used to establish proper myofibrillar order during larval and adult myofibrillogenesis.

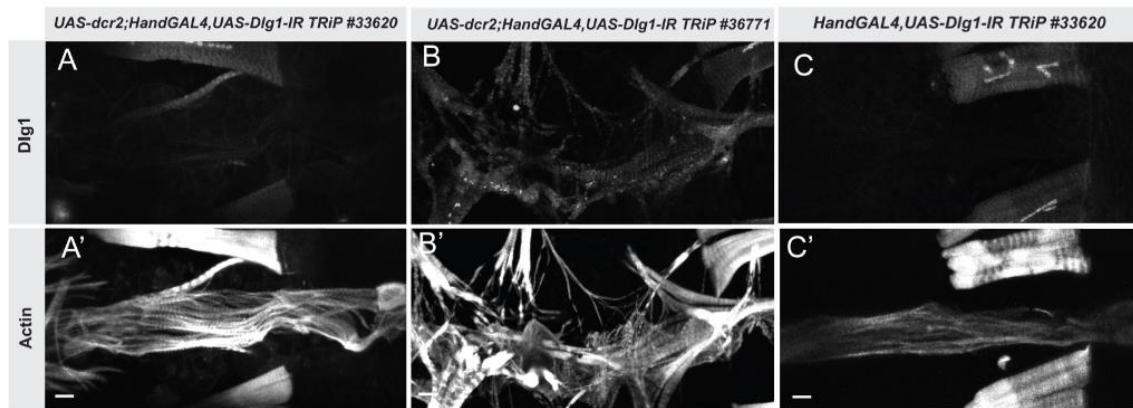


**Figure 25** When *Dlg1* is knocked-down with additional hairpins, myofibril arrangement is also disturbed

Knock-down phenotype of *Dlg1* using hairpins (#33620, #36771) from the Harvard TRiP RNAi resource crossed to the *UAS-dcr2;HandGAL4* driver line results in highly disturbed myofibrillar arrangement (A', B'). This effect is also observed without *dcr2* and myofibrillar arrangement is highly disturbed (C'). Scale bars: 100µm

Chromosome / Insert Position: X: 11285436

Gene diagram based on genome release 5



-Insert Position / Orientation

-CDS Start

-CDS End

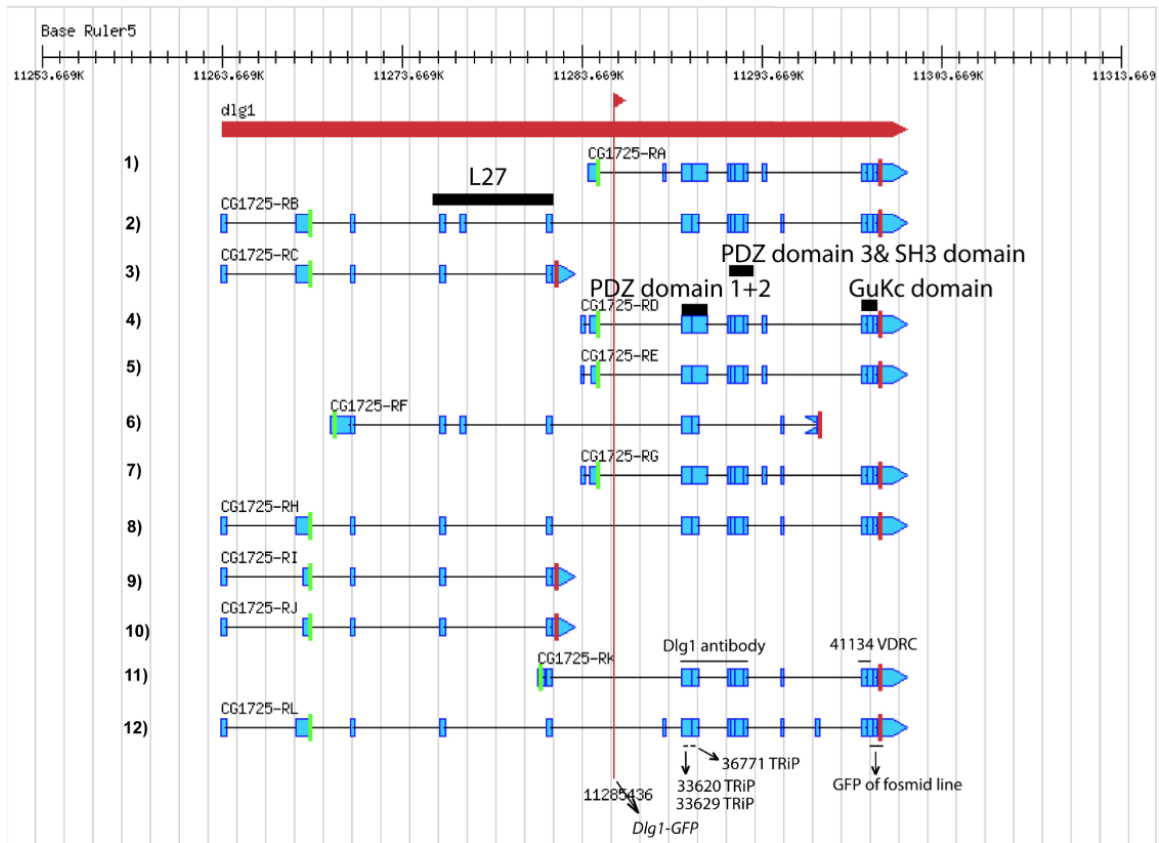


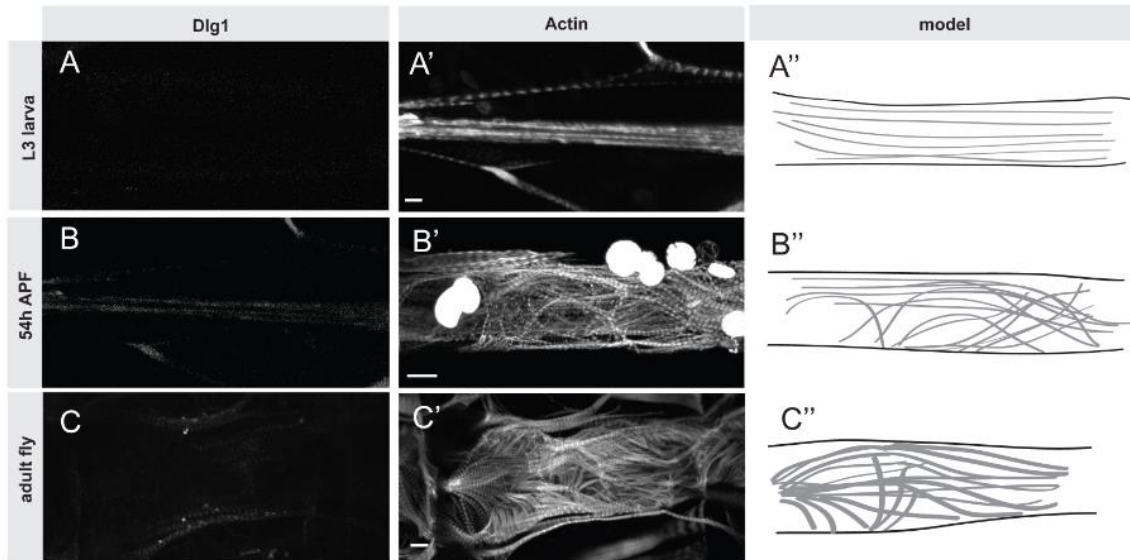
**Figure 26 Genomic structure of the *Dlg1* locus**

This map depicts the genomic loci encoding for the different Dlg1 protein isoforms (1-12). Above them, the protein domains are specified (L27, PDZ 1+2, PDZ 3, SH3, GuKc). The figure shows the epitope used for the Dlg1 antibody, as well as which parts of the mRNA are targeted by the 41134 RNAi line from VDRC and the TRiP lines #33620, #33629, and #36771. Furthermore, the GFP of the fosmid line is inserted at the C-terminal end of the long isoforms. The red flag indicates the position of the GFP insertion into the *Dlg1-GFP* trap line. This chart was downloaded from <http://flytrap.med.yale.edu>.

### 3.3.3 Cell junctions in *Dlg1* knock-down hearts

To mechanistically investigate the primary cause of the myofibril misarrangement phenotype in the *Dlg1* knock-down, I studied the localization of  $\beta$ PS integrin that in wild type is most prominently concentrated at the longitudinal cell-cell junction at which the myofibrils are anchored (Fig. 13). In contrast, upon *Dlg1* knock-down  $\beta$ PS integrin accumulates at the transverse cell-cell junction that anchors the wrongly oriented

myofibrils (Fig. 28). Thus, not only myofibril orientation but also  $\beta$ PS integrin localization is shifted to the transverse cell-cell junction.  $\beta$ PS integrin staining at the costameric Z-disc coincides with the new myofibril running direction (asterisk Fig. 28 B'). In conclusion, the localization of  $\beta$ PS integrin is dependent on Dlg1, suggesting that it acts upstream of integrins to polarize the cell. Integrin mislocalization most likely causes the myofibrillar misarrangement.



D Quantification of the larval phenotype

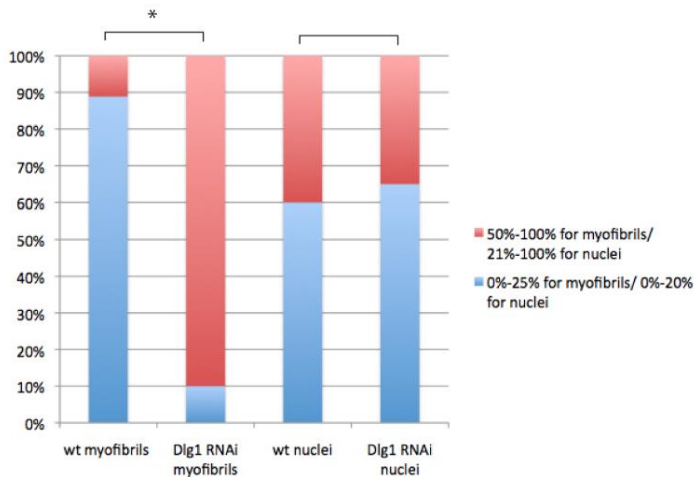


**Figure 27 The *Dlg1* phenotype arises at larval and pupal stages**

The *Dlg1* knock-down is shown with *UAS-dcr2;UAS-Dlg1-IR 41134;HandGAL4* at the larval L3 (A-A''), the 54h APF (B-B'') and the adult time point (C-C''). Actin stainings (A'- C'') as well as models of myofibrillar arrangement (A''- C'') show myofibrillar misarrangement at larval and pupal stages (compare to Fig. 11 and 17 for wild type). Quantification results for L3 wild type genotype and L3 RNAi genotype

are shown both for myofibrillar arrangement and nuclear positioning (D). Significance values were calculated using a one-tailed Fisher's Exact Test. Effects of *Dlg1* knock-down on myofibrillar arrangement are highly significant (indicated by an asterisk;  $p < 0.0001$ ), but not on nuclear positioning ( $p = 0.5$ ). Scale bars:  $100\mu\text{m}$

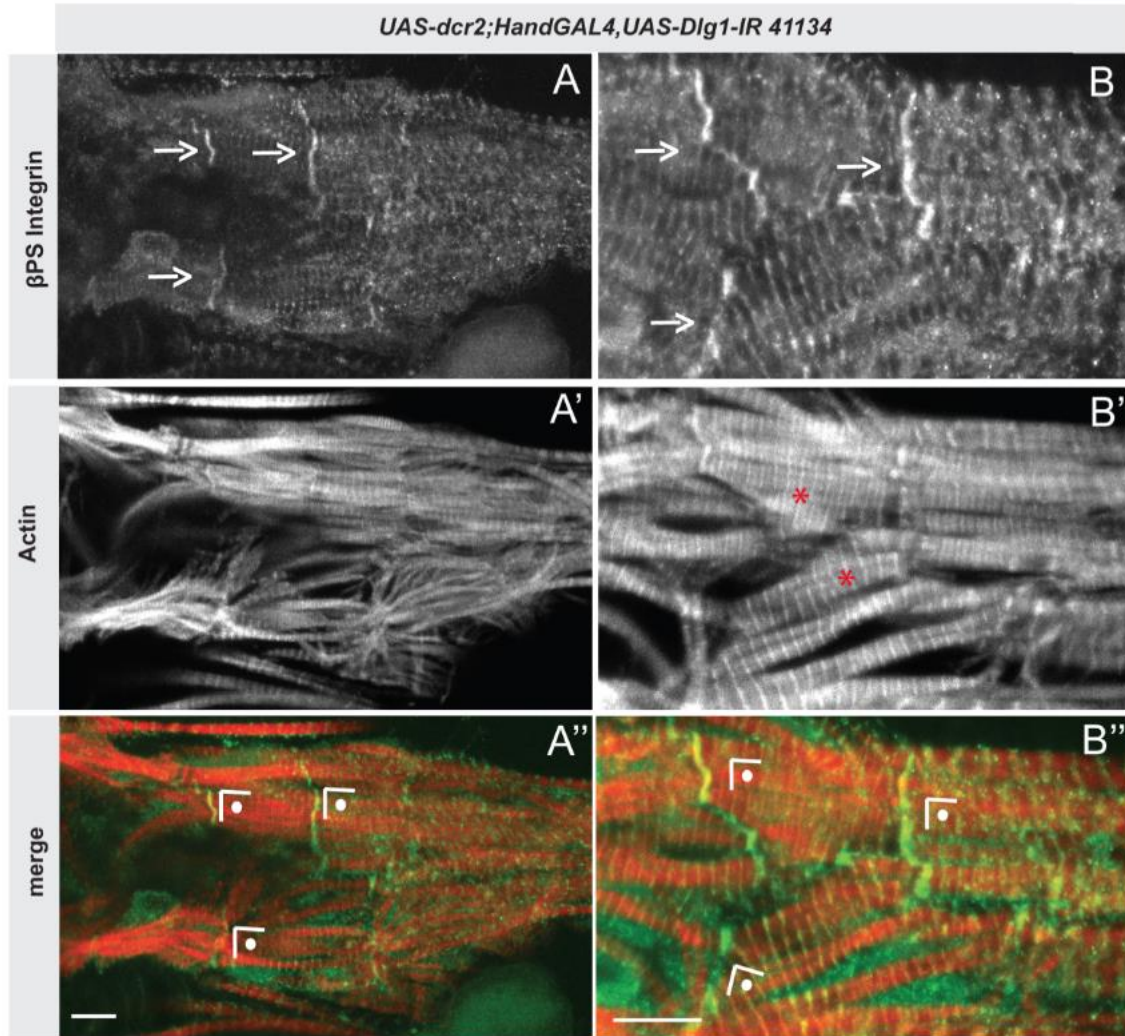


**Figure 28 Integrin localization in the *Dlg1* knock-down heart**

When *Dlg1* is knocked-down by crossing the *UAS-Dlg1-IR 41134* line to *UAS-dcr2;HandGAL4*, the longitudinal  $\beta\text{PS}$  integrin pool (A, B) is shifted by  $90^\circ$  (right angle symbols in A'' and B'') compared to the wild type situation (Fig. 13).  $\beta\text{PS}$  integrin remains at the costameres (red asterisks in B'). Scale bars:  $100\mu\text{m}$

To achieve a better understanding of how the cardiomyocytes are connected to each other in the *Dlg1* knock-down, I took a closer look at the cell-cell junctions (Fig. 29). Some cardiomyocytes lost the longitudinal junction completely, as no longitudinally

arranged  $\beta$ PS integrin was detected on the ventral side of the heart. Instead, only transverse junctions could be found.

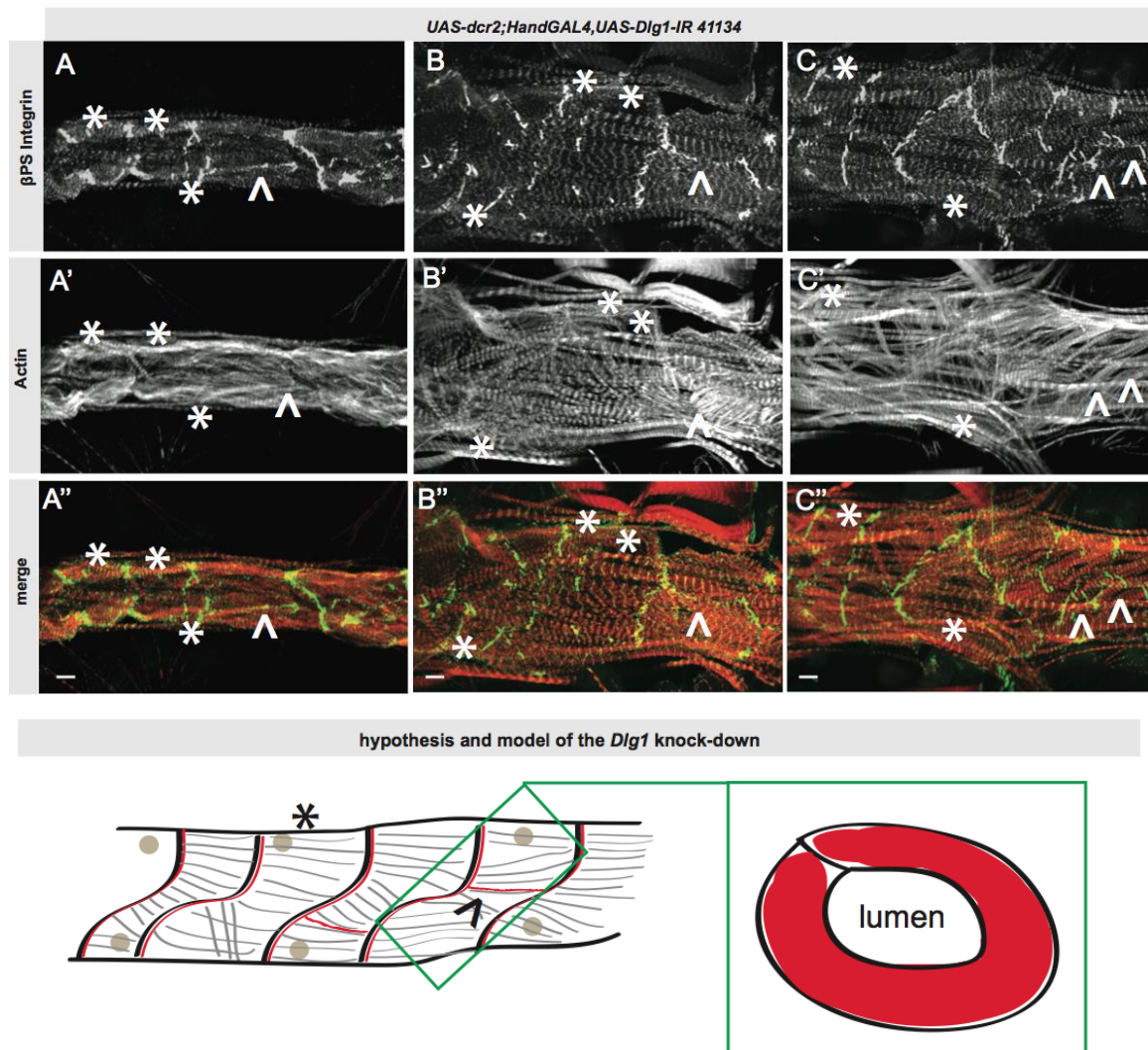


**Figure 29 Cell junctions in the *Dlg1* knock-down heart**

*Dlg1* knock-down hearts were stained for  $\beta$ PS integrin (A, B, C, green) and actin (A', B', C', red). Cardiomyocytes without a longitudinal cell-cell junction are marked with an asterisk. However, there are also some longitudinal cell-cell junctions left (marked by an arrowhead). They do not display the strong  $\beta$ PS integrin staining that can be found in the wild type but instead a faint one. Comparing Fig. 29 A to B and C, it becomes obvious that the heart is thinner in case the cellular rearrangement phenotype is more severe. The model of the ventral side of the heart that is shown below suggests an autocellular junction for the cardiomyocytes that possess a longitudinal cell-cell junction cell (membrane in black,  $\beta$ PS integrin pool in red, nuclei in brown, compare to wild type model in Fig. 13). Scale bars: 100 $\mu$ m

However, sometimes a faint  $\beta$ PS integrin localization was detected at the proper longitudinal cell-cell junctional locus (arrowheads). Thus, in the *Dlg1* knock-down heart, different connections inbetween cardiomyocytes are present.

Pericardin (*prc*) is a cardiac ECM protein that can bind to integrin and was recently found to be essential for the adhesion between heart tube and pericardial cells. It is secreted by embryonic cardiomyocytes and by fat body cells in the larva (Drechsler et al., 2013). In *prc* mutants, larval hearts show integrin mislocalization and a myofibrillar misarrangement phenotype, similar to the *Dlg1* loss-of-function phenotype. Thus, we were wondering if *prc* might be controlled by *Dlg1* in any way. Therefore, I analyzed adult wild type and *Dlg1* knock-down hearts by *prc* staining (Fig. 30 A, B). However, no obvious change in the *prc* pattern could be detected, suggesting that *prc* is not a downstream component of *Dlg1* within a hypothetical myofibril arrangement pathway.

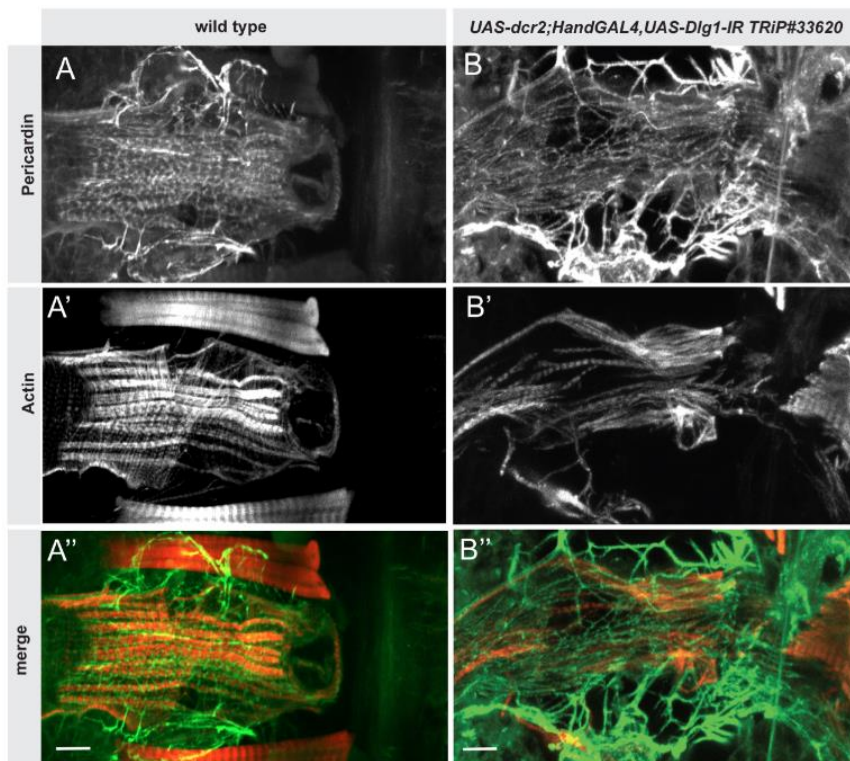


**Figure 30** The ECM protein pericardin is still normally distributed around the adult heart in the *Dlg1* knock-down

Dissections of wild type and *Dlg1* knock-down hearts were stained for pericardin (A, B, green) and actin (A', B', red). Scale bars: 100 $\mu$ m

### 3.4 Functional investigation of a genomic fosmid library in heart

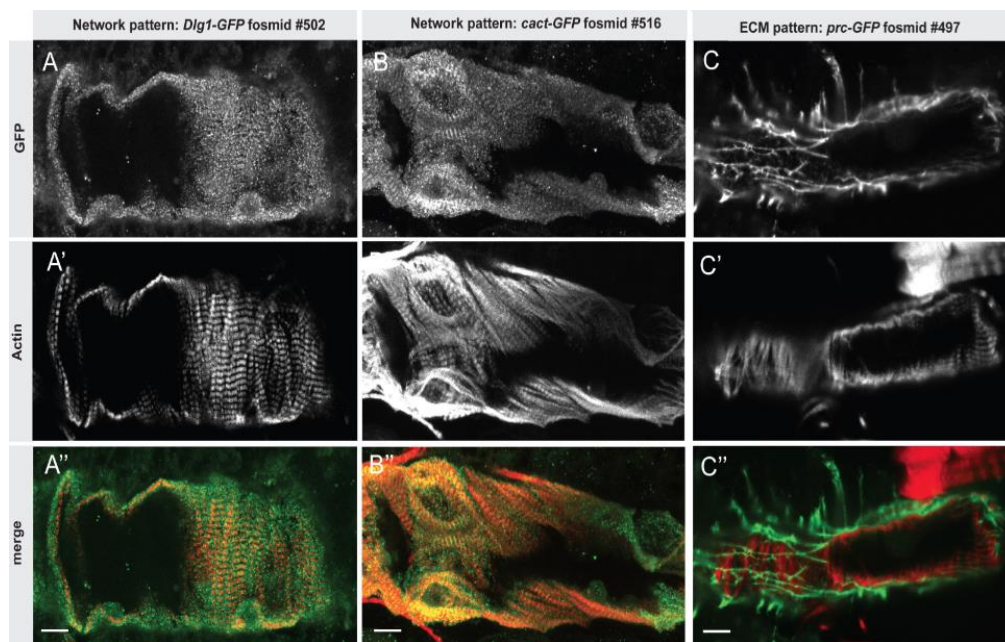
Complementary to my functional analysis, I participated in the characterization of a transgenic fosmid library resource (Table 1 and Fig. 31). This library consists of fosmid clones that harbour a genomic insert of about 40kb including at least one entire gene unit, which had been tagged by GFP with recombineering techniques (Ejsmont et al., 2009). I selected transgenic lines for 80 of these genes and tested their expression and localization in the heart and abdominal muscles of wild type adults. I was able to find four main expression patterns: 1) The expected network pattern was found for the *Dlg1* fosmid (Fig. 31 A) and unexpectedly, for the *cact* fosmid (Fig. 31 B). 2) An ECM localization found for the *prc* fosmid which is tightly localized around the cardiomyocytes facing the pericardial cells (Fig. 31 C). Both patterns are entirely consistent with my antibody stainings, suggesting that the GFP fusion will be fully functional. 3) As expected, a sarcomeric pattern was detected for *Mhc* (Fig. 31 D) and *Prm* (Table 1). 4) A nuclear pattern for the *Hand-GFP* fosmid (Fig. 31 E). Hand-GFP was found in the nuclei of the pericardial cells and cardiomyocytes, suggesting that the *Hand-GFP* fusion is functional. Further analyses of the twelve fosmid lines that showed a GFP signal can be found in Table 1.

These findings emphasize the importance and applicability of the fosmid source in *Drosophila* heart research and can now be used to investigate the myofibrillar phenotype of the *Dlg1* knock-down in greater detail.

fosmid	strong GFP signal	weak GFP signal	cell type expression	localization
Dlg1 #502	x		CM	T-tubules
Prc #497	x		ECM	ECM
Mhc #501	x		CM, AM	sarcomeres
Mhc #519	x		CM, AM	sarcomeres
Hand #10163	x		CM, PC	nucleus
Prm #475	x		CM, AM	sarcomeres
CG32667 #463	x		PC	vesicles
LanA1 #574		x	CM, PC, AM	ECM
LanB1 #681		x	CM, PC, AM	ECM
CG12391 #10036		x	CM, PC, AM, fat	nucleus
Cact #516		x	CM	sarcomeres
CG5625 #57		x	PC	cytoplasm

**Table 1 Evaluation of the cardiac fosmid screen**

Expression patterns for the 12 positive fosmid lines out of a screen of 80 fosmid lines in total. Further analysis includes the strength of the GFP signal and the cell type expression. CM: cardiomyocytes, PC: pericardial cells, ECM: extracellular matrix, AM: abdominal muscles, fat: fat tissue.



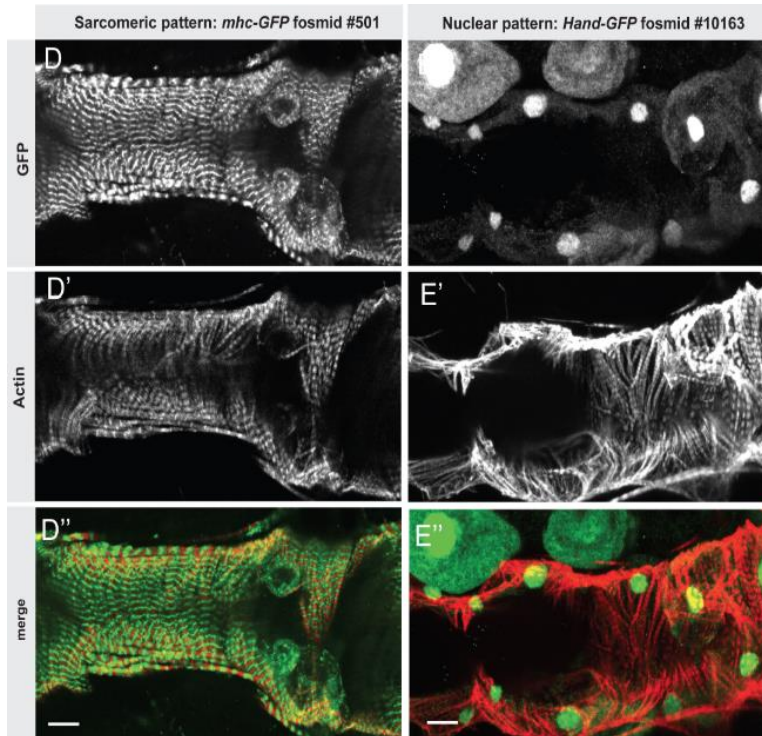


**Figure 31 GFP-tagged fosmid clones show expected localization patterns in adult heart**

Five fosmid lines (Dlg1: A- A'', Cact: B- B'', Prc: C- C'', Mhc: D- D'', Hand: E- E'') were stained for GFP at the adult stage (A-E) to test the GFP expression and localization. Four different morphological expression patterns could be detected: network-like for Dlg1 and Cact, ECM for Prc, sarcomeric for Mhc, and nuclear for Hand. Scale bars: 100 $\mu$ m

## 4. Discussion

This study investigated the genetic requirements for normal adult heart morphogenesis in *Drosophila melanogaster* with a focus on myofibrillar arrangement. It identified a novel and essential role for *Dlg1* in proper myofibril arrangement during heart development in larvae and pupae. The absence of *Dlg1* during these stages leads to a non-functional heart in adult flies.

The protein *Dlg1* is well known to play an important role in establishing epithelial polarity in various higher organisms (Bilder and Perrimon, 2000). In *Drosophila* epithelia, it builds a complex with *Lgl* and *Scrib* which is located at the basolateral cell membrane with a concentration at the septate junction, whereas *Crumbs*, *Par3*, *Par6* and *aPKC* are restricted to the apical membrane domain (Woods and Bryant, 1991; Petronczki and Knoblich, 2000; Wodarz et al., 2000; Bilder et al., 2002). In *Dlg1* mutants, epithelial polarity is disturbed and as a consequence, these cells divide abnormally fast and invade adjacent tissues (Woods et al., 1996; Goode and Perrimon, 1997; Woods et al., 1997; Woodhouse et al., 1998). Also, mitotic spindle position was found to be abnormal (Bergstralh et al., 2013).

### 4.1 Loss of *Dlg1* in heart by RNAi results in major heart defects

In order to identify genes that are responsible for myofibrillar organization of the heart, I tested a number of candidate genes that had been found to play an important role in *Drosophila* muscle and are known regulators of epithelial polarity (Schnorrer et al., 2010). By applying heart-specific RNAi using a *Hand-GAL4* line in combination with *UAS-dcr2* I was able to knock-down genes in the heart only, thus avoiding lethality at an earlier stage, e.g. as caused by an essential role of a given gene in epidermis or body muscle. In *Drosophila*, a functional heart is not required for eclosion of the adult fly, thus even a highly abnormal heart leads to viable adults. This strategy identified *Dlg1* as a key candidate for arranging myofibrils in the heart. When knocked-down during heart development, myofibrils in the larval as well as in the adult heart lose their circular orientation within the two opposing cardiomyocyte rows which form the heart tube. Instead they now run in an anterior-posterior direction. Thus, their orientation is changed by approximately 90°. As the circular orientation of the myofibrils is important for proper

heart contractions, the *Dlg1* knock-down heart displays major contraction defects, now contracting in anterior-posterior direction.

It would be interesting to test if these functional heart defects lead to a shorter life span as has been demonstrated for other functional heart defects (Ocorr et al., 2007).

#### **4.2 Probing the specificity of the *Dlg1* RNAi phenotype**

As all strong *Dlg1* mutant alleles are lethal at embryonic or early larval stages due to major epithelial polarity defects, this study solely relies on RNA interference. An important caveat of RNAi is a potential off-target effect, that is caused by knocking-down a gene other than the intended target gene (Ma et al., 2006). Two widely applied methods to confirm RNAi specificity use genetic rescue constructs to rescue the knock-down phenotype or different RNAi constructs to confirm the phenotype. Unfortunately, the rescue experiment of the *UAS-Dlg1-IR* #41134 phenotype by overexpression of *UAS-Dlg1-GFP* was not successful, because Dlg1-GFP was not expressed in the presence of the hairpin (Fig. 24). Most likely, *UAS-Dlg1-IR* #41134 is so effective that it also prevents the expression of the GFP-coupled Dlg1 as the hairpin target sequence is present in Dlg1-GFP.

Importantly, the second strategy to show specificity was successful. I was able to confirm the aforementioned myofibril phenotype caused by *UAS-Dlg1-IR* #41134 with three further *Dlg1* RNAi lines from the Harvard Transgenic RNAi Resource Project (#33620, #33629, #36771). #33620, #33629 are derived from the same construct whereas #36771 targets a different region of *Dlg1*. Thus, in total I detected a myofibrillar arrangement phenotype in three different *UAS-Dlg1-IR* constructs, which clearly demonstrates the specificity of the knock-down phenotype.

#### **4.3 Dlg1 redirects myofibrils together with integrins**

The mechanism by which Dlg1 instructs the arrangement of myofibrils most likely involves integrins. In the wild type adult heart tube,  $\beta$ PS integrin is not only localized at the costameres anchoring the sarcomeric Z-discs to the ECM (Fig. 15) but also at the longitudinal cell-cell junction between the two opposing cardiomyocyte rows (Fig. 13). Hence, the adult *Drosophila* heart contains two pools of integrins: one at the costamere

(called “costameric”) and one at the longitudinal cell-cell junctions (called “longitudinal”).

While it was established, that costameres anchor the myofibrils at the membrane of each cardiomyocyte to the surrounding ECM in vertebrate heart (Danowski et al., 1992; Quach and Rando, 2006; Legate et al., 2009), not much attention had been paid to the longitudinal integrin pool in heart before this work. This integrin pool is located at the ends of the myofibrils and thus appears to be a key factor for their organization and orientation. This hypothesis is strongly supported by the *Dlg1* knock-down phenotype. Upon *Dlg1* knock-down, the arrangement of both the myofibrils and the longitudinal  $\beta$ PS integrin pool are shifted by about  $90^\circ$  (Fig. 28). This means that both the localization of the longitudinal  $\beta$ PS integrin pool and the arrangement of the circular myofibrils are dependent on Dlg1. These findings suggest that the myofibrils are oriented by the longitudinal  $\beta$ PS integrin pool in wild type hearts, whereas the costameric integrin pool is anchoring the myofibrils at the outer cell surface in both wild type and *Dlg1-IR* (Fig. 28).

#### **4.4 The *Dlg1* phenotype arises during heart development in larvae and pupae**

RNAi knock-down of *Dlg1* leads to myofibril orientation defects during larval and pupal development (Fig. 27). Already the few myofibrils present in the larval heart are preferentially oriented in anterior to posterior direction along the heart tube instead of the circular pattern. Furthermore, all newly formed myofibrils during pupal development appear in anterior to posterior direction. This shows that Dlg1 is required for the first steps of myofibril assembly, possibly by somehow distinguishing the anterior-posterior axis of the cardiomyocyte from the circular axis.

How could Dlg1 achieve this mechanistically? Considering the premyofibril model of myofibril assembly (Sparrow and Schöck, 2009), Dlg1 might be required to recruit terminal Z-discs or their precursors preferentially to the longitudinal cell-cell junction of the heart tube. However, this hypothesis is only partially supported by our data. During larval stages when only few myofibrils are present in the aorta of the larval heart no clear localization of Dlg1 can be found at the longitudinal cell-cell junction. Dlg1 rather localizes along the myofibrils. However,  $\beta$ PS integrin is located at the ends of the myofibrils. At the critical time period in pupae when all the adult myofibrils are

organized de novo, Dlg1 is found in membraneous patches in close association with the newly forming myofibrils at 46h APF at the cell cortex. Although an obvious concentration at the longitudinal cell-cell junction could not be detected with our current resolution, small amounts of Dlg1 are present at the site of myofibril origin. Thus, our working hypothesis is that Dlg1 differentially polarizes the cardiomyocyte membrane and possibly recruits the first premyofibrils to the longitudinal cell-cell junction which then mature into the well organized circular myofibrils of the adult heart.

#### **4.5 How does Dlg1 link to integrins?**

In epithelia, integrins are often found at the basal side of the cells facing the basal lamina whereas Dlg1 is located along the entire basolateral membrane domain with a concentration at the septate junctions (Woods and Bryant, 1991; Bilder et al., 2002). In the adult cardiomyocytes I found Dlg1 to form clusters around the myofibrils including the area of the longitudinal  $\beta$ PS integrin pool. However, the overlap of both stainings was rather small. Integrins are single transmembrane proteins with the largest part of the molecule localized outside of the cell and just a short tail facing the cytoplasm (Legate et al., 2009). It seems unlikely that Dlg1 binds directly to  $\beta$ PS integrin but could do so by interacting with other known proteins of the integrin signalling complex like talin, kindlin or vinculin (Legate et al., 2009; Moser et al., 2009). In the future, biochemical purification experiments involving mass spectrometry might shed light on the question to which partners Dlg1 binds in the *Drosophila* heart.

In epithelia, Dlg1 binds to Scrib and Lgl. Interestingly, Scrib helps to localize the apical determinants to the apical side of the cell. However, localization of basolateral determinants like Dlg1 remains largely unchanged upon loss of Scrib (Bilder and Perrimon, 2000). I also investigated Scrib and Lgl distribution with antibodies and tested RNAi knock-down, but neither of them showed a clear staining in the heart nor had a heart phenotype upon knock-down (data not shown). Thus, it is likely that a different complex, analogous to the Scrib-Dlg1-Lgl complex in epithelia (Woods and Bryant, 1991; Bilder et al., 2002) or the Dlg1-Pins-Mud complex in the follicular epithelium (Bergstralh et al., 2013), is required to mediate Dlg1 function in the heart.

#### 4.6 Comparing cardiac polarity to epithelial polarity

The heart does not exhibit a clear epithelial morphology in which each cuboidal cell possesses an apical and a basolateral membrane domain with a basal anchor to a basement membrane. However, the heart does have important polar morphological features. Each cardiomyocyte displays a luminal membrane facing the heart lumen and an abluminal membrane facing the surrounding ECM and pericardial cells. The myofibrils are located close to the abluminal membrane, whereas the nuclei are positioned at the luminal side, forming a little membrane bulb (Fig. 12). The myofibrils originate from the longitudinal cell-cell junction, but not from the transverse ones. These features suggest a cardiac polarity with compartmentalization of the plasma membrane similar to epithelial cells. In addition, this study identified a different membrane domain in the heart: the T-tubular system that is strongly enriched with amphiphysin and Dlg1, suggesting that Dlg1 has additional functions apart from organizing the myofibrils in the heart.

What is the consequence of the changed polarity in the *Dlg1* knock-down adult heart? The working model shown in Figure 29 suggests a partial loss of the longitudinal junctions in *Dlg1* knock-down hearts. This model is built from the absence of a clear junction in the most severe cases using  $\alpha$ -spectrin or integrin markers, suggesting that the overall cell positions in the opposing two rows of cardiomyocytes might be rearranged. This phenotype would obviously be directly linked to the changed myofibril orientation phenotype and thus needs further careful investigation. As the nuclear positions of the cardiomyocytes are not changed significantly and at least a small lumen in cross-sections of *Dlg1* knock-down hearts is detectable (data not shown), it appears possible that *Dlg1* knock-down cardiomyocytes might form single cellular tubes via autocellular junctions as has been observed in *Drosophila* trachea (Lubarsky and Krasnow, 2003).

#### 4.7 A function for pericardial cells in myofibril organization

Interestingly, a recent publication found that loss of *pericardin* (*prc*) leads to a very similar phenotype as loss of *Dlg1* (Drechsler et al., 2013). In *prc* mutants, the polarity of the myofibrils is also changed to an anterior-posterior orientation. Prc is a collagen-like ECM protein located between pericardial cells and cardiomyocytes. It is proposed to bind to the extracellular part of integrin dimers and could thus signal from outside to organize

integrins (Chartier et al., 2002). It will be interesting to investigate if Dlg1 and  $\beta$ PS integrin localization is also changed in the *prc* mutants. I investigated *prc* distribution in *Dlg1-IR* adult hearts and found that *prc* is still present (Fig. 30). However it will be important to study *prc* localization during myofibrillogenesis in pupal stages in wild type and *Dlg1-IR* in order to test if *prc* and Dlg1 act within a similar pathway to organize myofibrils.

#### 4.8 Dlg1 and cardiomyopathies

Human cardiomyopathies are important public health problems. They can be inherited or sporadic. The two most frequent types include hypertrophic cardiomyopathy (HCM) and dilated cardiomyopathy (DCM) which affects most people suffering from cardiomyopathy (Sussman et al., 1998; Parvari and Levitas, 2012). HCM is characterized by hypertrophy of the left ventricle as well as myofibrillar disarray (Parvari and Levitas, 2012), the latter being exactly what was observed in the *Dlg1* knock-down situation (Fig. 22). Many genes have been found to be mutated in human cardiomyopathies, among them the gene of the  $\beta$ -myosin heavy chain (Geisterfer-Lowrance et al., 1990) and of  $\alpha$ -tropomyosin and cardiac troponin T (Thierfelder et al., 1994). Other mutations cover genes for cardiac troponin I and C,  $\alpha$ -cardiac actin, regulatory myosin light chain, cardiac myosin-binding protein C, titin, and several Z-disc proteins (Morimoto, 2007). However, the search for additional genes involved in the pathogenesis of cardiomyopathies is still ongoing.

Since *Dlg1* is conserved to humans (Cho et al., 1992; Lue et al., 1994; Brenman et al., 1996; Makino et al., 1997; Hanada et al., 2000) and homologs have been found in the dog, mouse and human heart (Jesaitis and Goodenough, 1994; Makino et al., 1997; Yamazaki et al., 2010), it is possible that a *Dlg1* homolog might also serve as an important factor for cardiac myofibrillar arrangement in humans.

From a morphological point of view, the longitudinal integrin pool in *Drosophila* heart is similar in morphology and function to the intercalated disc in vertebrates (Figs. 6 and 7) (Forbes and Sperelakis, 1985; Bellin, 2001; Franke et al., 2006; Capetanaki et al., 2007). This again stresses the importance of this study's findings for human cardiac pathologies.

#### **4.9 The fosmid library: a valuable resource for *Drosophila* biology**

Transgenic GFP-tagged fosmid clones are a powerful tool to investigate the expression, localization and function of certain genes. I participated in the characterization of 80 GFP-tagged genes as well as the investigation of their expression and localization in the adult *Drosophila* heart. I showed here that a wide range of protein classes from transcription factors to sarcomeric proteins and ECM components are expressed in the expected cell type and localized to the correct subcellular compartment. This suggests that transgenic fusion proteins are also functional. Ultimately these fosmids need to be crossed into the mutant background to prove that they rescue the mutant phenotype. We expect that this resource will be highly valuable for the *Drosophila* community as it can have multiple applications, such as live imaging, protein localization and complex purification procedures.

## 5. Materials and Methods

### Fly work

Fly stocks were kept at 18°C, RNAi crosses at 27°C and other crosses at 25°C. Flies were flipped every 3-4 weeks.

For pupal dissections, 0h APF pupae were staged and kept until aged to 46h APF or 54h APF at 27°C.

### Fly strains

As a genetic driver for the experiments, I used *HandCGAL4* (Sellin et al., 2006) which leads to cardiomyocyte-specific expression of the hairpin.

I crossed the *UAS-dcr2;HandGAL4* line with the *UAS-Dlg1-IR* (TF 41134, VDRC, hairpin sequence can be found at <http://stockcenter.vdrc.at>) or the TRiP RNAi lines #33620, #33629, #36771 (Flockhart et al., 2011 and [www.flyrnai.org](http://www.flyrnai.org)) for all knock-down experiments. For some stainings, the *Dlg1-GFP* trap line YC0005 from the FlyTrap project was used (<http://flytrap.med.yale.edu>) (Morin et al., 2001; Kelso, 2004). Crossing the *UAS-dcr2;HandGAL4* line with the *w*-flies served as the control.

For the rescue stock I crossed the *UAS-Dlg1-IR* line #41134 with a fly line containing *UAS-Dlg1-GFP* (gift from Barry Thompson).

### Dissections

All dissections were conducted in Phosphate Buffered Saline (PBS) with 0.1% Triton-X (Roth).

10x PBS was produced by adding 80g of NaCl (Merck), 2g of KCl (Merck), 14.4g of Na<sub>2</sub>HPO<sub>4</sub> (Merck) and 2.4g of KH<sub>2</sub>PO<sub>4</sub> (Merck) to 1L of distilled water and adjusting the pH to 7.4.

L3 larvae were first pinned down with Austerlitz Insect pins at the anterior and posterior end with their dorsal side pointing down. Next, I cut the ventral side open from anterior to posterior and pinned down the left and right tissue rims with Austerlitz insect pins again. Then, I carefully removed muscle, fat and gut tissue such that the heart is dissected cleanly.

For pupae, I first cut the pupal case with the tip of the forceps carefully from anterior to posterior and then freed the pupa. I pinned it down at the thorax with the dorsal side downwards. Then I cut the posterior-most part of the abdomen open and cut along the left

and right from posterior to anterior. Afterwards I cut the whole ventral part of the abdomen and carefully removed muscle, fat and gut tissue such that the heart is dissected cleanly.

Adult dissections were performed like the pupal ones except the removal of the pupal case.

Instruments that were used for dissection include scissors (Fine Science Tools) and forceps (neo Lab).

For cross sections, flies were fixed in 4% paraformaldehyde (Merck) in PBS overnight and were washed the next morning and embedded in 7% ultra pure agarose (Invitrogen). Then they were sectioned on the Leica VT1000 S vibrating blade microtome.

### **Antibodies and Immunostainings**

First, the dissected samples were fixed for 15min in relaxing solution, containing 20mM sodium phosphate (Merck), 5mM magnesium chloride (Sigma-Aldrich), 0.1% Triton-X (Roth), 5mM ATP (Merck), 5mM EGTA (Sigma-Aldrich) and 4% PFA (Sigma-Aldrich). After three washing steps with PBS 0.1% Tween (Serva Electrophoresis GmbH), samples were blocked with 3% goat serum in PBS 0.1% Triton-X for 3 hours. Then one or more of the following antibodies were applied at 4°C over night:

Mouse anti-Dlg1 (DSHB, clone 4F3), used at 1:500

Mouse anti- $\alpha$ -spectrin (DSHB, clone 3A9), used at 1:2

Mouse anti- $\beta$ PS integrin (DSHB, clone CF.6G11), used at 1:250

Rabbit anti-GFP (amsbio), used at 1:1000

Rabbit anti-Tin (gift from Manfred Frasch), used at 1:1000

Rabbit anti-zormin (gift from Belinda Bullard), used at 1:50

Rabbit anti-SERCA (gift from Mani Ramaswami), used at 1:500

The next morning, three washing steps with PBS 0.1% Triton-X followed. Afterwards, samples were stained with phalloidin and anti-rabbit or mouse secondary antibodies coupled to Alexa 488 or 568 (Life Technologies, Invitrogen Molecular Probes) for 3 hours. After washing, samples were embedded using Vectashield with DAPI (Vector Laboratories Inc.) as mounting medium.

### **Quantification of myofibrillar misarrangement and nuclear positioning**

Myofibrillar misarrangement was assessed by the percentage of misarrangement, 0% and 25% misarrangement being considered as wild type and 50%, 75%, and 100% being classified as a misarrangement phenotype. Example pictures of each percentage are shown in Figure 23.

Nuclear misarrangement is expressed by the percentage of single nuclei present in the evaluated hearts: Wild type cardiac morphology is characterized by two opposing rows of cardiomyocytes, meaning that opposing nuclei are facing each other, thus forming pairs. In every heart, the total number of nuclei was counted and the ones which are not part of a pair meaning that are not facing another nucleus were counted. The percentage of single nuclei was calculated by dividing both numbers. Here, 0% to 20% single nuclei were considered as wild type and 21% to 100% single nuclei as phenotype.

A one-tailed Fisher's Exact Test was used to calculate the significance values, with a p-value smaller than 0.05 being significant.

Sample numbers were as follows:

n (adult wt hearts for myofibrillar arrangement): 14

n (adult *Dlg1* RNAi hearts for myofibrillar arrangement): 20

n (adult wt hearts for nuclear positioning): 15

n (adult *Dlg1* RNAi hearts for nuclear positioning): 15

n (L3 wt hearts for myofibrillar arrangement): 18

n (L3 *Dlg1* RNAi hearts for myofibrillar arrangement): 20

n (L3 wt hearts for nuclear positioning): 20

n (L3 *Dlg1* RNAi hearts for nuclear positioning): 20

### **Imaging**

All images were taken using the Zeiss LSM780. Image processing was performed with ImageJ and Photoshop. Plot profiles were done in ImageJ, too.

## 6. References

- Anderson, J.M. (1996). Cell signalling: MAGUK magic. *Curr. Biol.* 6, 382–384.
- Bellin, R.M. (2001). Synemin may function to directly link muscle cell intermediate filaments to both myofibrillar Z-lines and costameres. *J. Biol. Chem.* 276, 32330–32337.
- Beltrami, C.A., Finato, N., Rocco, M., Feruglio, G.A., Puricelli, C., Cigola, E., Sonnenblick, E.H., Olivetti, G., and Anversa, P. (1995). The cellular basis of dilated cardiomyopathy in humans. *J. Mol. Cell. Cardiol.* 27, 291–305.
- Bergstralh, D.T., Lovegrove, H.E., and St Johnston, D. (2013). Discs large links spindle orientation to apical-basal polarity in *Drosophila* epithelia. *Curr. Biol.* 23, 1707–1712.
- Bernstein, E., Caudy, A.A., Hammond, S.M., and Hannon, G.J. (2001). Role for a bidentate ribonuclease in the initiation step of RNA interference. *Nature* 409, 363–366.
- Bilder, D., and Perrimon, N. (2000). Localization of apical epithelial determinants by the basolateral PDZ protein Scribble. *Nature* 403, 676–680.
- Bilder, D., Schober, M., and Perrimon, N. (2002). Integrated activity of PDZ protein complexes regulates epithelial polarity. *Nat. Cell Biol.* 5, 53–58.
- Bischof, J., Maeda, R.K., Hediger, M., Karch, F., and Basler, K. (2007). An optimized transgenesis system for *Drosophila* using germ-line-specific phiC31 integrases. *Proc. Natl. Acad. Sci. USA* 104, 3312–3317.
- Brand, A.H., and Perrimon, N. (1993). Targeted gene expression as a means of altering cell fates and generating dominant phenotypes. *Development* 118, 401–415.
- Brenman, J.E., Christopherson, K.S., Craven, S.E., McGee, A.W., and Bredt, D.S. (1996). Cloning and characterization of postsynaptic density 93, a nitric oxide synthase interacting protein. *J. Neurosci.* 16, 7407–7415.
- Bryant, P.J.P. (1996). Junction genetics. *Dev. Genet.* 20, 75–90.
- Buckingham, M., Meilhac, S., and Zaffran, S. (2005). Building the mammalian heart from two sources of myocardial cells. *Nat. Rev. Genet.* 6, 826–837.
- Budnik, V.V., Koh, Y.H.Y., Guan, B.B., Hartmann, B.B., Hough, C.C., Woods, D.D., and Gorczyca, M.M. (1996). Regulation of synapse structure and function by the *Drosophila* tumor suppressor gene *dlg*. *Neuron* 17, 14–14.
- Burkart, C., Qiu, F., Brendel, S., Benes, V., Hååg, P., Labeit, S., Leonard, K., and Bullard, B. (2007). Modular proteins from the *Drosophila* *sallimus* (*sls*) gene and their expression in muscles with different extensibility. *J. Mol. Biol.* 367, 953–969.
- Capetanaki, Y., Bloch, R.J., Kouloumenta, A., Mavroidis, M., and Psarras, S. (2007).

Muscle intermediate filaments and their links to membranes and membranous organelles. *Exp. Cell Res.* 313, 2063–2076.

Chartier, A., Zaffran, S., Astier, M., Sémériva, M., and Gratecos, D. (2002). Pericardin, a *Drosophila* type IV collagen-like protein is involved in the morphogenesis and maintenance of the heart epithelium during dorsal ectoderm closure. *Development* 129, 3241–3253.

Cho, K.O.K., Hunt, C.A.C., and Kennedy, M.B.M. (1992). The rat brain postsynaptic density fraction contains a homolog of the *Drosophila* discs-large tumor suppressor protein. *Neuron* 9, 929–942.

Crawford, G.L., and Horowitz, R. (2011). Scaffolds and chaperones in myofibril assembly: putting the striations in striated muscle. *Biophys. Rev.* 3, 25–32.

Danowski, B.A., Imanaka-Yoshida, K., Sanger, J.M., and Sanger, J.W. (1992). Costameres are sites of force transmission to the substratum in adult rat cardiomyocytes. *J. Cell Biol.* 118, 1411–1420.

Dietzl, G., Chen, D., Schnorrer, F., Su, K.-C., Barinova, Y., Fellner, M., Gasser, B., Kinsey, K., Oppel, S., Scheiblaue, S., et al. (2007). A genome-wide transgenic RNAi library for conditional gene inactivation in *Drosophila*. *Nature* 448, 151–156.

Dlugosz, A.A., Antin, P.B., Nachmias, V.T., and Holtzer, H. (1984). The relationship between stress fiber-like structures and nascent myofibrils in cultured cardiac myocytes. *J. Cell Biol.* 99, 2268–2278.

Drechsler, M., Schmidt, A.C., Meyer, H., and Paululat, A. (2013). The conserved ADAMTS-like protein lonely heart mediates matrix formation and cardiac tissue integrity. *PLoS Genet.* 9, e1003616.

Du, A., Sanger, J.M., and Sanger, J.W. (2008). Cardiac myofibrillogenesis inside intact embryonic hearts. *Dev. Biol.* 318, 236–246.

Du, A., Sanger, J.M., Linask, K.K., and Sanger, J.W. (2003). Myofibrillogenesis in the first cardiomyocytes formed from isolated quail precardiac mesoderm. *Dev. Biol.* 257, 382–394.

Ejsmont, R.K., Sarov, M., Winkler, S., Lipinski, K.A., and Tomancak, P. (2009). A toolkit for high-throughput, cross-species gene engineering in *Drosophila*. *Nat. Methods* 6, 435–437.

Fire, A., Xu, S., Montgomery, M.K., Kostas, S.A., Driver, S.E., and Mello, C.C. (1998). Potent and specific genetic interference by double-stranded RNA in *Caenorhabditis elegans*. *Nature* 391, 806–811.

Flockhart, I.T., Booker, M., Hu, Y., McElvany, B., Gilly, Q., Mathey-Prevot, B., Perrimon, N., and Mohr, S.E. (2011). FlyRNAi.org--the database of the *Drosophila* RNAi

screening center: 2012 update. *Nucleic Acids Res.* *40*, D715–D719.

Forbes, M.S., and Sperelakis, N. (1985). Intercalated discs of mammalian heart: a review of structure and function. *Tissue Cell* *17*, 605–648.

Franke, W.W., Borrmann, C.M., Grund, C., and Pieperhoff, S. (2006). The area composita of adhering junctions connecting heart muscle cells of vertebrates. I. Molecular definition in intercalated disks of cardiomyocytes by immunoelectron microscopy of desmosomal proteins. *Eur. J. Cell Biol.* *85*, 69–82.

Fujita, H., Nedachi, T., and Kanzaki, M. (2007). Accelerated de novo sarcomere assembly by electric pulse stimulation in C2C12 myotubes. *Exp. Cell Res.* *313*, 1853–1865.

Fyrberg, E.A., and Goldstein, L.S. (1990). The *Drosophila* cytoskeleton. *Annu. Rev. Cell Biol.* *6*, 559–596.

Geisterfer-Lowrance, A.A., Kass, S., Tanigawa, G., Vosberg, H.P., McKenna, W., Seidman, C.E., and Seidman, J.G. (1990). A molecular basis for familial hypertrophic cardiomyopathy: a beta cardiac myosin heavy chain gene missense mutation. *Cell* *62*, 999–1006.

Goode, S., and Perrimon, N. (1997). Inhibition of patterned cell shape change and cell invasion by Discs large during *Drosophila* oogenesis. *Genes Dev.* *11*, 2532–2544.

Grimes, A.C., Durán, A.C., Sans-Coma, V., Hami, D., Santoro, M.M., and Torres, M. (2010). Phylogeny informs ontogeny: a proposed common theme in the arterial pole of the vertebrate heart. *Evol. Dev.* *12*, 552–567.

Groth, A.C., Fish, M., Nusse, R., and Calos, M.P. (2004). Construction of transgenic *Drosophila* by using the site-specific integrase from phage phiC31. *Genetics* *166*, 1775–1782.

Haag, T.A., Haag, N.P., Lekven, A.C., and Hartenstein, V. (1999). The role of cell adhesion molecules in *Drosophila* heart morphogenesis: faint sausage, shotgun/DE-cadherin, and laminin A are required for discrete stages in heart development. *Dev. Biol.* *208*, 56–69.

Hammond, S.M. (2001). Argonaute2, a link between genetic and biochemical analyses of RNAi. *Science* *293*, 1146–1150.

Han, Z. (2005). Hand is a direct target of Tinman and GATA factors during *Drosophila* cardiogenesis and hematopoiesis. *Development* *132*, 3525–3536.

Hanada, N., Makino, K., Koga, H., Morisaki, T., Kuwahara, H., Masuko, N., Tabira, Y., Hiraoka, T., Kitamura, N., Kikuchi, A., et al. (2000). NE-dlg, a mammalian homolog of *Drosophila* dlg tumor suppressor, induces growth suppression and impairment of cell adhesion: possible involvement of down-regulation of beta-catenin by NE-dlg expression.

Int. J. Cancer 86, 480–488.

Holtzer, H., Hijikata, T., Lin, Z.X., Zhang, Z.Q., Holtzer, S., Protasi, F., Franzini-Armstrong, C., and Sweeney, H.L. (1997). Independent assembly of 1.6 microns long bipolar MHC filaments and I-Z-I bodies. *Cell Struct. Funct.* 22, 83–93.

Hough, C.D., Woods, D.F., Park, S., and Bryant, P.J. (1997). Organizing a functional junctional complex requires specific domains of the *Drosophila* MAGUK Discs large. *Genes Dev.* 11, 3242–3253.

Humbert, P., Russell, S., and Richardson, H. (2003). Dlg, Scribble and Lgl in cell polarity, cell proliferation and cancer. *Bioessays* 25, 542–553.

Huxley, H., Hanson, J. (1954). Changes in the cross-striations of muscle during contraction and stretch and their structural interpretation. *Nature* 173, 973–976.

Izant, J.G., and Weintraub, H. (1984). Inhibition of thymidine kinase gene expression by anti-sense RNA: a molecular approach to genetic analysis. *Cell* 36, 1007–1015.

Jesaitis, L.A., and Goodenough, D.A. (1994). Molecular characterization and tissue distribution of ZO-2, a tight junction protein homologous to ZO-1 and the *Drosophila* discs-large tumor suppressor protein. *J. Cell Biol.* 124, 949–961.

Kelso, R.J. (2004). Flytrap, a database documenting a GFP protein-trap insertion screen in *Drosophila melanogaster*. *Nucleic Acids Res.* 32, 418D–420.

Kornau, H.C., Schenker, L.T., Kennedy, M.B., and Seeburg, P.H. (1995). Domain interaction between NMDA receptor subunits and the postsynaptic density protein PSD-95. *Science* 269, 1737–1740.

Kölsch, V., and Paululat, A. (2002). The highly conserved cardiogenic bHLH factor Hand is specifically expressed in circular visceral muscle progenitor cells and in all cell types of the dorsal vessel during *Drosophila* embryogenesis. *Dev. Genes Evol.* 212, 473–485.

Legate, K.R., Wickstrom, S.A., and Fassler, R. (2009). Genetic and cell biological analysis of integrin outside-in signaling. *Genes Dev.* 23, 397–418.

Lehmacher, C., Abeln, B., and Paululat, A. (2012). The ultrastructure of *Drosophila* heart cells. *Arthropod Struct. Dev.* 41, 459–474.

Liu, Q. (2003). R2D2, a bridge between the initiation and effector steps of the *Drosophila* RNAi pathway. *Science* 301, 1921–1925.

Lo, P.C.H., Skeath, J.B., Gajewski, K., Schulz, R.A., and Frasch, M. (2002). Homeotic genes autonomously specify the anteroposterior subdivision of the *Drosophila* dorsal vessel into aorta and heart. *Dev. Biol.* 251, 307–319.

Lubarsky, B., and Krasnow, M.A. (2003). Tube morphogenesis: making and shaping biological tubes. *Cell* *112*, 19–28.

Lue, R.A., Marfatia, S.M., Branton, D., and Chishti, A.H. (1994). Cloning and characterization of hdlg: the human homologue of the *Drosophila* discs large tumor suppressor binds to protein 4.1. *Proc. Natl. Acad. Sci. USA* *91*, 9818–9822.

Ma, Y., Creanga, A., Lum, L., and Beachy, P.A. (2006). Prevalence of off-target effects in *Drosophila* RNA interference screens. *Nature* *443*, 359–363.

Mahoney, Z.X., Sammut, B., Xavier, R.J., Cunningham, J., Go, G., Brim, K.L., Stappenbeck, T.S., Miner, J.H., and Swat, W. (2006). Discs-large homolog 1 regulates smooth muscle orientation in the mouse ureter. *Proc. Natl. Acad. Sci. USA* *103*, 19872–19877.

Makino, K., Kuwahara, H., Masuko, N., Nishiyama, Y., Morisaki, T., Sasaki, J., Nakao, M., Kuwano, A., Nakata, M., Ushio, Y., et al. (1997). Cloning and characterization of NE-dlg: a novel human homolog of the *Drosophila* discs large (dlg) tumor suppressor protein interacts with the APC protein. *Oncogene* *14*, 2425–2433.

Medioni, C., Astier, M., Zmojdian, M., Jagla, K., and Sémériva, M. (2008). Genetic control of cell morphogenesis during *Drosophila melanogaster* cardiac tube formation. *J. Cell Biol.* *182*, 249–261.

Migaud, M., Charlesworth, P., Dempster, M., Webster, L.C., Watabe, A.M., Makhinson, M., He, Y., Ramsay, M.F., Morris, R.G., Morrison, J.H., et al. (1998). Enhanced long-term potentiation and impaired learning in mice with mutant postsynaptic density-95 protein. *Nature* *396*, 433–439.

Molina, M.R., and Cripps, R.M. (2001). Ostia, the inflow tracts of the *Drosophila* heart, develop from a genetically distinct subset of cardial cells. *Mech. Dev.* *109*, 51–59.

Monier, B., Astier, M., Sémériva, M., and Perrin, L. (2005). Steroid-dependent modification of Hox function drives myocyte reprogramming in the *Drosophila* heart. *Development* *132*, 5283–5293.

Morimoto, S. (2007). Sarcomeric proteins and inherited cardiomyopathies. *Cardiovasc. Res.* *77*, 659–666.

Morin, X., Daneman, R., Zavortink, M., and Chia, W. (2001). A protein trap strategy to detect GFP-tagged proteins expressed from their endogenous loci in *Drosophila*. *Proc. Natl. Acad. Sci. USA* *98*, 15050–15055.

Moser, M., Legate, K.R., Zent, R., and Fässler, R. (2009). The tail of integrins, talin, and kindlins. *Science* *324*, 895–899.

Na, J., Musselman, L.P., Pendse, J., Baranski, T.J., Bodmer, R., Ocorr, K., and Cagan, R. (2013). A *Drosophila* model of high sugar diet-induced cardiomyopathy. *PLoS Genet.* *9*,

e1003175.

Ni, J.-Q., Zhou, R., Czech, B., Liu, L.-P., Holderbaum, L., Yang-Zhou, D., Shim, H.-S., Tao, R., Handler, D., Karpowicz, P., et al. (2011). A genome-scale shRNA resource for transgenic RNAi in *Drosophila*. *Nat. Methods* 8, 405–407.

Noorman, M., van der Heyden, M.A.G., van Veen, T.A.B., Cox, M.G.P.J., Hauer, R.N.W., de Bakker, J.M.T., and van Rijen, H.V.M. (2009). Cardiac cell–cell junctions in health and disease: Electrical versus mechanical coupling. *J. Mol. Cell. Cardiol.* 47, 23–31.

Ocorr, K., Perrin, L., Lim, H.-Y., Qian, L., Wu, X., and Bodmer, R. (2007). Genetic control of heart function and aging in *Drosophila*. *Trends Cardiovasc. Med.* 17, 177–182.

Parrish, S., Fleenor, J., Xu, S., Mello, C., and Fire, A. (2000). Functional anatomy of a dsRNA trigger: differential requirement for the two trigger strands in RNA interference. *Mol. Cell* 6, 1077–1087.

Parvari, R., and Levitas, A. (2012). The mutations associated with dilated cardiomyopathy. *Biochem. Res. Int.* 2012, 1–12.

Perriard, J.-C., Hirschy, A., and Ehler, E. (2003). Dilated cardiomyopathy: a disease of the intercalated disc? *Trends Cardiovasc. Med.* 13, 30–38.

Perrin, L., Monier, B., Ponzelli, R., Astier, M., and Sémériva, M. (2004). *Drosophila* cardiac tube organogenesis requires multiple phases of Hox activity. *Dev. Biol.* 272, 419–431.

Person, V., Kostin, S., Suzuki, K., Labeit, S., and Schaper, J. (2000). Antisense oligonucleotide experiments elucidate the essential role of titin in sarcomerogenesis in adult rat cardiomyocytes in long-term culture. *J. Cell Sci.* 113 Pt 21, 3851–3859.

Petronczki, M.M., and Knoblich, J.A.J. (2000). DmPAR-6 directs epithelial polarity and asymmetric cell division of neuroblasts in *Drosophila*. *Nat. Cell Biol.* 3, 43–49.

Prall, O.W.J., Menon, M.K., Solloway, M.J., Watanabe, Y., Zaffran, S., Bajolle, F., Biben, C., McBride, J.J., Robertson, B.R., Chaulet, H., et al. (2007). An Nkx2-5/Bmp2/Smad1 negative feedback loop controls heart progenitor specification and proliferation. *Cell* 128, 947–959.

Qian, L., Liu, J., and Bodmer, R. (2005). Slit and Robo control cardiac cell polarity and morphogenesis. *Curr. Biol.* 15, 2271–2278.

Quach, N.L., and Rando, T.A. (2006). Focal adhesion kinase is essential for costamerogenesis in cultured skeletal muscle cells. *Dev. Biol.* 293, 38–52.

Razzaq, A. (2001). Amphiphysin is necessary for organization of the excitation-contraction coupling machinery of muscles, but not for synaptic vesicle endocytosis in

*Drosophila*. *Genes Dev.* *15*, 2967–2979.

Reim, I., and Frasch, M. (2010). Genetic and genomic dissection of cardiogenesis in the *Drosophila* model. *Pediatr. Cardiol.* *31*, 325–334.

Reuver, S.M., and Garner, C.C. (1998). E-cadherin mediated cell adhesion recruits SAP97 into the cortical cytoskeleton. *J. Cell Sci.* *111* ( Pt 8), 1071–1080.

Roignant, J.Y. (2003). Absence of transitive and systemic pathways allows cell-specific and isoform-specific RNAi in *Drosophila*. *RNA* *9*, 299–308.

Santiago-Martínez, E., Soplop, N.H., and Kramer, S.G. (2006). Lateral positioning at the dorsal midline: Slit and Roundabout receptors guide *Drosophila* heart cell migration. *Proc. Natl. Acad. Sci. USA* *103*, 12441–12446.

Schnorrer, F., Schönbauer, C., Langer, C.C.H., Dietzl, G., Novatchkova, M., Schernhuber, K., Fellner, M., Azaryan, A., Radolf, M., Stark, A., et al. (2010). Systematic genetic analysis of muscle morphogenesis and function in *Drosophila*. *Nature* *464*, 287–291.

Sellin, J., Albrecht, S., Kölsch, V., and Paululat, A. (2006). Dynamics of heart differentiation, visualized utilizing heart enhancer elements of the *Drosophila melanogaster* bHLH transcription factor Hand. *Gene Expr. Patterns* *6*, 360–375.

Sipido, K.R., Acsai, K., Antoons, G., Bito, V., and Macquaide, N. (2012). T-tubule remodelling and ryanodine receptor organization modulate sodium-calcium exchange. *Adv. Exp. Med. Biol.* *961*, 375–383.

Soeller, C., and Cannell, M.B. (1999). Examination of the transverse tubular system in living cardiac rat myocytes by 2-photon microscopy and digital image-processing techniques. *Circ. Res.* *84*, 266–275.

Sparrow, J.C., and Schöck, F. (2009). The initial steps of myofibril assembly: integrins pave the way. *Nat. Rev. Mol. Cell Biol.* *10*, 293–298.

Sussman, M.A., Welch, S., Cambon, N., Klevitsky, R., Hewett, T.E., Price, R., Witt, S.A., and Kimball, T.R. (1998). Myofibril degeneration caused by tropomodulin overexpression leads to dilated cardiomyopathy in juvenile mice. *J. Clin. Invest.* *101*, 51–61.

Thierfelder, L., Watkins, H., MacRae, C., Lamas, R., McKenna, W., Vosberg, H.P., Seidman, J.G., and Seidman, C.E. (1994). Alpha-tropomyosin and cardiac troponin T mutations cause familial hypertrophic cardiomyopathy: a disease of the sarcomere. *Cell* *77*, 701–712.

Thomas, U., Ebitsch, S., Gorczyca, M., Koh, Y.H., Hough, C.D., Woods, D., Gundelfinger, E.D., and Budnik, V. (2000). Synaptic targeting and localization of disc-large is a stepwise process controlled by different domains of the protein. *Curr. Biol.* *10*,

1108–1117.

Thomas, U.U., Phannavong, B.B., Müller, B.B., Garner, C.C.C., and Gundelfinger, E.D.E. (1997). Functional expression of rat synapse-associated proteins SAP97 and SAP102 in *Drosophila* dlg-1 mutants: effects on tumor suppression and synaptic bouton structure. *Mech. Dev.* *62*, 161–174.

Tokuyasu, K.T. (1989). Immunocytochemical studies of cardiac myofibrillogenesis in early chick embryos. III. Generation of fasciae adherentes and costameres. *J. Cell Biol.* *108*, 43–53.

Vincent, S.D., and Buckingham, M.E. (2010). How to make a heart: the origin and regulation of cardiac progenitor cells. *Curr. Top. Dev. Biol.* *90*, 1-41.

Volk, T., Fessler, L.I., and Fessler, J.H. (1990). A role for integrin in the formation of sarcomeric cytoarchitecture. *Cell* *63*, 525–536.

Wodarz, A., Ramrath, A., Grimm, A., and Knust, E. (2000). *Drosophila* atypical protein kinase C associates with Bazooka and controls polarity of epithelia and neuroblasts. *J. Cell Biol.* *150*, 1361–1374.

Woodhouse, E., Hersperger, E., and Shearn, A. (1998). Growth, metastasis, and invasiveness of *Drosophila* tumors caused by mutations in specific tumor suppressor genes. *Dev. Genes Evol.* *207*, 542–550.

Woods, D.F., and Bryant, P.J. (1991). The discs-large tumor suppressor gene of *Drosophila* encodes a guanylate kinase homolog localized at septate junctions. *Cell* *66*, 451–464.

Woods, D.F., Hough, C., Peel, D., Callaini, G., and Bryant, P.J. (1996). Dlg protein is required for junction structure, cell polarity, and proliferation control in *Drosophila* epithelia. *J. Cell Biol.* *134*, 1469–1482.

Woods, D.F., Wu, J.W., and Bryant, P.J. (1997). Localization of proteins to the apico-lateral junctions of *Drosophila* epithelia. *Dev. Genet.* *20*, 111–118.

Yamazaki, T., Walchli, S., Fujita, T., Ryser, S., Hoshijima, M., Schlegel, W., Kuroda, S., and Maturana, A.D. (2010). Splice variants of Enigma homolog, differentially expressed during heart development, promote or prevent hypertrophy. *Cardiovasc. Res.* *86*, 374–382.

Zaffran, S. (2002). Early signals in cardiac development. *Circ. Res.* *91*, 457–469.

Zaffran, S. (2006). Cardioblast-intrinsic Tinman activity controls proper diversification and differentiation of myocardial cells in *Drosophila*. *Development* *133*, 4073–4083.

Zamore, P.D., Tuschl, T., Sharp, P.A., and Bartel, D.P. (2000). RNAi: double-stranded RNA directs the ATP-dependent cleavage of mRNA at 21 to 23 nucleotide intervals. *Cell*

101, 25–33.

Zeitouni, B., Sénatore, S., Séverac, D., Aknin, C., Sémériva, M., and Perrin, L. (2007). Signalling pathways involved in adult heart formation revealed by gene expression profiling in *Drosophila*. *PLoS Genet* 3, e174.

Zito, K., Fetter, R.D., Goodman, C.S., and Isacoff, E.Y. (1997). Synaptic clustering of Fasciclin II and Shaker: essential targeting sequences and role of Dlg. *Neuron* 19, 1007–1016.

## 7. Acknowledgements

I thank Dr. Frank Schnorrer for giving me the opportunity to decipher the mechanisms of morphology development in the *Drosophila* heart. It was an interesting challenge to explore this field of muscle biology as the first and only person in the Schnorrer lab. Many thanks to all other members of the Schnorrer lab, too. Furthermore, I would like to mention the good times we spent outside the lab, in particular our wine tastings and various Christmas dinners at Frank's place.

I am thankful to my doctor father Prof. Dr. Stefan Jentsch who gave me invaluable input during my Thesis Advisory Committee meetings.

I am moreover thankful to Prof. Dr. Heinrich Leonhardt as second examiner of this thesis. My further thanks go to Prof. Dr. Ute Vothknecht, PD Dr. Anna Friedl, Prof. Dr. Angelika Böttger and Prof. Dr. George Boyan for being members of my thesis committee.

I thank Prof. Dr. Reinhard Fässler for stimulating scientific discussions in the Department Seminars and for hosting our group in his department at the MPI of Biochemistry.

I would also like to thank Prof. Dr. Achim Paululat for being a member of my Thesis Advisory Committee and for sharing his excellent scientific and methodological ideas due to his great insight and experience in the field of *Drosophila* cardiac biology. I am also thankful to Bettina Abeln, PhD student in the Paululat lab, for sharing my interest in questions about the *Drosophila* heart and fruitful scientific discussions.

Many thanks go to Prof. Dr. Andreas Wodarz, Prof. Dr. Achim Paululat, Prof. Dr. Manfred Frasch and Dr. Barry Thompson for generously sharing flies and reagents. We also thank the TRiP at Harvard Medical School (NIH/NIGMS R01-GM084947) for providing some of the transgenic RNAi fly stocks used in this study.

My great gratitude appertains to the Boehringer Ingelheim Fonds- Stiftung für medizinische Grundlagenforschung for invaluable ideal and financial support during my PhD time. I would like to especially mention the beautiful and adventurous hikes we set forth on during the Hirscheegg summer seminar 2012 and the scientific discussions and non-scientific conversations we had.

I would also like to thank Dr. Hans-Joerg Schaeffer, Dr. Ingrid Wolf and Maximiliane Reif for their admirable organization of the IMPRS-LS PhD program.

Irish Pub Radio and Klassikradio made many hours of fly work and other routine work enjoyable.

My colleague and dear friend Irene Ferreira completes the acknowledgement section: I have been greatly gifted to share with you wonderful times and conversations, scientific and non-scientific, inside and outside the lab. Special thanks for your help with the nuclear and myofibrillar quantifications.